AD-A045 931 FOREIGN TECHNOLOGY DIV WRIGHT-PATTERSON AFB OHIO F/G 20/4
HYDRODYNAMICS OF LIFTING SURFACES (SELECTED ARTICLES).(U)
MAY 77

UNCLASSIFIED FTD-ID(RS)T-0784-77 NL

1 OF 2
ADA
045931

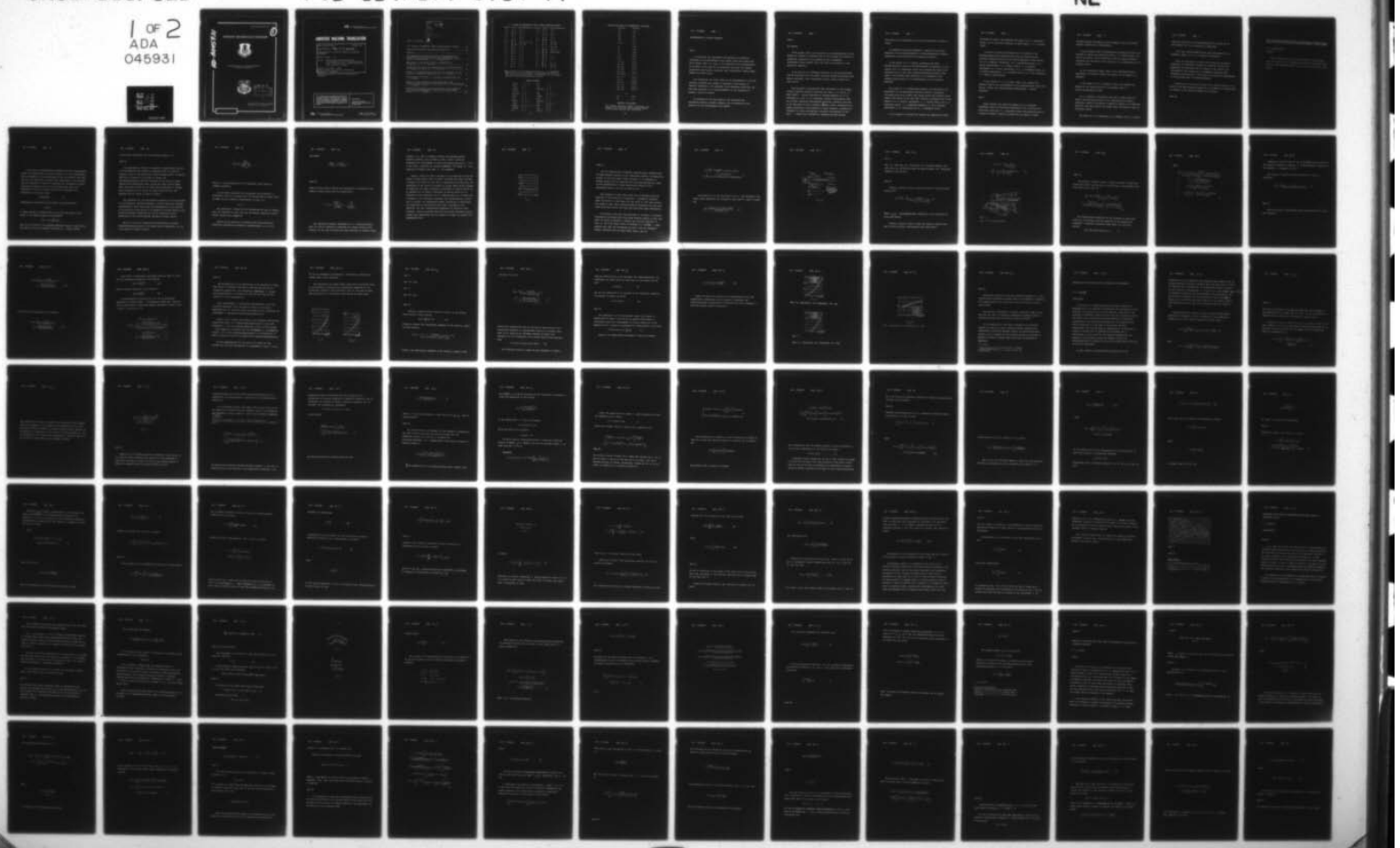

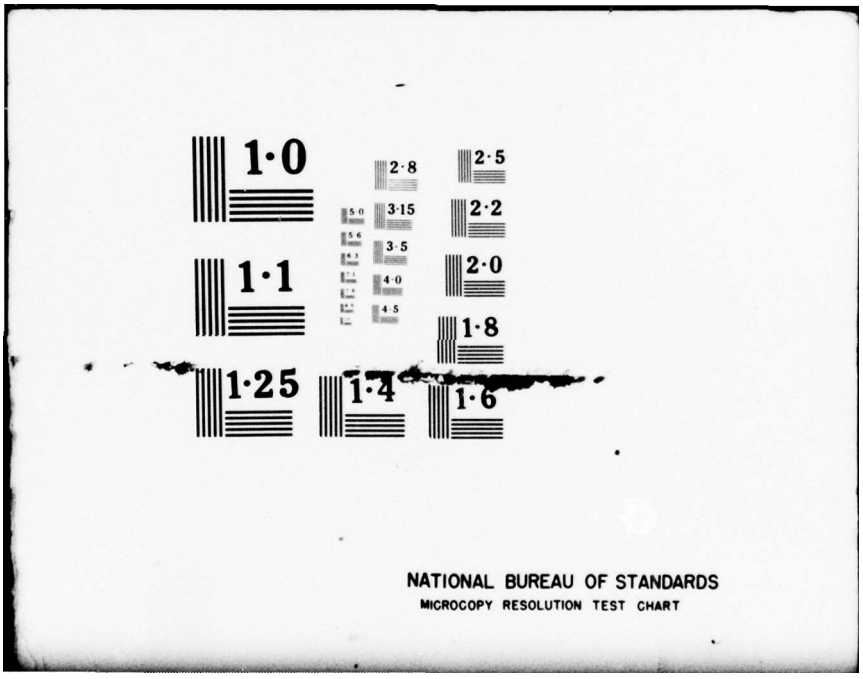
1·0
1·1
1·25
2·8
3·15
3·5
4·0
4·5
5·0
5·6
6·3
2·5
2·2
2·0
1·8
1·4
1·6
NATIONAL BUREAU OF STANDARDS
MICROCOPY RESOLUTION TEST CHART

FTD-ID(RS)T-0784-77

FOREIGN TECHNOLOGY DIVISION

HYDRODYNAMICS OF LIFTING SURFACES
(SELECTED ARTICLES)

Approved for public release;
distribution unlimited.

UNEDITED MACHINE TRANSLATION

FTD-ID(RS)T-0784-77 27 May 1977

MICROFICHE NR: FTD-77-C-000626

HYDRODYNAMICS OF LIFTING SURFACES (SELECTED ARTICLES)

English pages: 161

Source: Gidroaerodinamika Nesushchikh Poverkhnostey, Izd-vo "Naukova Dumka" Kiev, 1966, pp. 1-4, 24-46, 56-69, 188-191, 223-229, 254-274

Country of origin: USSR
This document is a machine translation
Requester: FTD/PDRS

Approved for public release, distribution unlimited

PREPARED BY:

TRANSLATION DIVISION
FOREIGN TECHNOLOGY DIVISION
WP-AFB, OHIO.

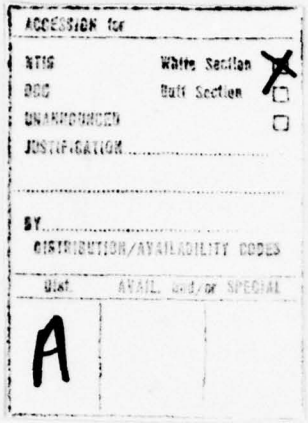

Table of contents

U. S. BOARD ON GEOGRAPHIC NAMES TRANSLITERATION SYSTEM

Block	Italic	Transliteration	Block	Italic	Transliteration
А а	*А а*	A, a	Р р	*Р р*	R, r
Б б	*Б б*	B, b	С с	*С с*	S, s
В в	*В в*	V, v	Т т	*Т т*	T, t
Г г	*Г г*	G, g	У у	*У у*	U, u
Д д	*Д д*	D, d	Ф ф	*Ф ф*	F, f
Е е	*Е е*	Ye, ye; E, e*	Х х	*Х х*	Kh, kh
Ж ж	*Ж ж*	Zh, zh	Ц ц	*Ц ц*	Ts, ts
З з	*З з*	Z, z	Ч ч	*Ч ч*	Ch, ch
И и	*И и*	I, i	Ш ш	*Ш ш*	Sh, sh
Й й	*Й й*	Y, y	Щ щ	*Щ щ*	Shch, shch
К к	*К к*	K, k	Ъ ъ	*Ъ ъ*	"
Л л	*Л л*	L, l	Ы ы	*Ы ы*	Y, y
М м	*М м*	M, m	Ь ь	*Ь ь*	'
Н н	*Н н*	N, n	Э э	*Э э*	E, e
О о	*О о*	O, o	Ю ю	*Ю ю*	Yu, yu
П п	*П п*	P, p	Я я	*Я я*	Ya, ya

*ye initially, after vowels, and after ъ, ь; e elsewhere. When written as ë in Russian, transliterate as yë or ë. The use of diacritical marks is preferred, but such marks may be omitted when expediency dictates.

GREEK ALPHABET

Alpha	A	α		Nu	N	ν	
Beta	B	β		Xi	Ξ	ξ	
Gamma	Γ	γ		Omicron	O	o	
Delta	Δ	δ		Pi	Π	π	
Epsilon	E	ε		Rho	P	ρ	
Zeta	Z	ζ		Sigma	Σ	σ	ς
Eta	H	η		Tau	T	τ	
Theta	Θ	θ		Upsilon	T	υ	
Iota	I	ι		Phi	Φ	φ	
Kappa	K	κ		Chi	X	χ	
Lambda	Λ	λ		Psi	Ψ	ψ	
Mu	M	μ		Omega	Ω	ω	

RUSSIAN AND ENGLISH TRIGONOMETRIC FUNCTIONS

Russian	English
sin	sin
cos	cos
tg	tan
ctg	cot
sec	sec
cosec	csc
sh	sinh
ch	cosh
th	tanh
cth	coth
sch	sech
csch	csch
arc sin	$\sin^{-1}$
arc cos	$\cos^{-1}$
arc tg	$\tan^{-1}$
arc ctg	$\cot^{-1}$
arc sec	$\sec^{-1}$
arc cosec	$\csc^{-1}$
arc sh	$\sinh^{-1}$
arc ch	$\cosh^{-1}$
arc th	$\tanh^{-1}$
arc cth	$\coth^{-1}$
arc sch	sech^{-1}
arc csch	csch^{-1}
rot	curl
lg	log

GRAPHICS DISCLAIMER

All figures, graphics, tables, equations, etc. merged into this translation were extracted from the best quality copy available.

HYDRODYNAMICS OF LIFTING SURFACES.

In collection are represented the materials of scientific conference on the hydrodynamics high speeds, which was taking place 28-30 October 1965 in g. Kiev in the institute of the hydromechanics of AS UkSSR. In the work of the conference take part the leading specialists from Moscow, Leningrad, Kiev, Novosibirsk, Gorkiy, Kazan, Kharkov and other cities.

Are illuminated the urgent tasks of the hydrodynamics of lifting surfaces and bodies near screen or interface of the liquids of different densities in the presence of the developed cavitation, and also some questions of a reduction/descent in the resistance of medium to motion of bodies.

Is intended for the wide circle of the scientific and engineering workers, graduate students, who are occupied by the questions of the hydrodynamics high speeds.

Page 3.

The preface

28-30 October 1965 in the institute of the hydromechanics of the Academy of Sciences of Ukrainian SSR (g. Kiev) passes the scientific conference, dedicated to the problems of the contemporary hydrodynamics large speeds, which will draw the attention of wide scientific community.

In the work of the conference take part of 106 representatives from 45 organizations of the USSR, including leading specialists from Moscow, Leningrad, Kiev, Novosibirsk, Gorkiy, kazan, Kharkov and other cities.

From scientific organizations were represented to CSRI [ЦНИИ - Central Scientific Research Institute] im. acad. A. N. Krylov, to TsAGI [ЦАГИ - Central Institute of Aerohydrodynamics im. N. Ye Zhukovskiy im. Prof. N. Ye. Joukowski, Institut hydrodynamics WITH the AS USSR, Leningrad ship-building institute, Leningrad institute of the engineers of water transport, TsNIIMF, Gorkiy, Novosibirsk and Odessa institutes of the engineers of water transport, Kazansky and Kiyevskiy the state universities, institute the mechanics of MGU [МГУ - Moscow State University], Kazansky and Khar'kovskiy

institutes of the engineers of the civil aviation and a series of others.

At conference read and discussed 41 reports on the urgent questions of the aerohydrodynamics of high-speed/velocity objects, representing large theoretical and practical interest.

In the report of I. T. Yegorov (Leningrad) was made survey/coverage of works on the hydrodynamics of hydrofoil, in the reports of A. N. Panchenkova (Kiev) were examined the task of the unsteady motion of wing with alternating/variable distance from screen, are discussed some questions of the statement of the boundary-value problem of the hydrodynamics of the cavitating hydrofoil.

The report of K. K. Fedyaevskiy (Moscow) was dedicated to the examination of the approximate nonlinear theory of rectangular low-aspect-ratio wing, moving near liquid screen with Froude's large numbers. The motion of the wing near a screen is examined also in the reports of V. P. Shadrin (Leningrad), P. I. Zinchuk (Kiev), by A. N. Lukashenko (Kiev), V. I. Menshikov (Kharkov), E. of A. Paravyan (Leningrad), A. N. Panchenkova and A. I. Yukhimenko (Kiev).

To the dynamics of takeoff and landing the apparatuses, which

use effect of screen, was dedicated the report of V. I. Rudomanova (Kiev), but of the static stability of their motion - V. I. Koreleva (Kiev).

A series of reports was dedicated to the studies of the hydroaerodynamic wing characteristics and wing systems during different mode/conditions and the under conditions of their motion - Ya. of F. Parberova (Leningrad), Yu. M. Polishchuk (Kiev), V. B. Kurzin (Novosibirsk), S. I. Putilin (Kiev), G. V. Sobolyov (Leningrad), M. A. Basin (Leningrad), by A. I. Yukhimenko (Kiev), Ye. N. Grafova (Leningrad), V. G. Savchenko (Kiev), S. F. Orlov (Gorkiy), L. I. Maltsev (Novosibirsk).

In the reports of V. M. Ivchenko (Kiev) were examined the unsteady tasks of the hydrodynamics of the supercavitating bodies and carrier systems with application/use ETsVM [ЭЦВМ - digital computer].

Large interest will cause the reports of G. A. Riazanov (Leningrad) about the electrical simulation of the flow about the finite-span wings and V. V. Kopeyetskiy about the application/use of a method of magnetic models to account for the effect of blade

thickness during the design of screw propeller with the assigned pressure differential on blade/vanes.

To the boundary-layer calculations and profile wing drag in the presence of suction was dedicated report L. F. Kozlova (Kiev), the data on the effect vortex formation on the wing drag and body of revolution were presented in the report of A. M. Mkhitaryan and V. A. Fridland (Kiev).

On the experimental model tests of the high-speed/velocity apparatuses of different systems will impart in his reports E. G. Pasechnik.

In the report of Ye. P. Udartseva (Kiev) are examined the methods of the laminarization of the boundary layer of electro-hydrodynamical flows.

Yu. K. Biktimirov (Leningrad) will make a report about the special feature/peculiarities of the construction of velocity potential, caused by the motion of source in liquid, R. B. Nudel'man (Kharkov) will come forward with report about the motion of body in multilayer liquid.

The report of A. M. Mkhitaryan, V. S. Maximov and P. S. Laznyuk

(Kiev) was dedicated to the investigations of the flow of the semi-bounded slot jets, spreading in slipstream.

With short report/communications will come forward Ye. G. Sheshukov (kazan) and Yu. K. Biktimirov (Leningrad).

After the discussion of reports and rotting on the sums of conference is unanimously accepted the solution, in which was emphasized the importance and the urgency of the tasks of the hydrodynamics high speeds and is recommended conducting more widespread investigations in this field, including the investigation of the unsteady tasks of aerohydrodynamics.

Conference will note also certain lag of Soviet science in the field of the supercavitating wings and it recommends to develop works on research on the spatial problems of cavitation.

Page 24.

THE APPROXIMATE NONLINEAR THEORY OF RECTANGULAR LOW-ASPECT-RATIO WING, WHICH MOVES NEAR LIQUID SCREEN WITH FROUDE'S LARGE NUMBERS

K. K. Fedyayevskiy

(Moscow)

Work represents by itself the development of approximate nonlinear theory [2] of rectangular low-aspect-ratio wing, which moves in unbounded medium near liquid screen with Froude's large numbers.

If we from the experimentally determined value of torque/moment deduct the torque/moment of inertia nature, i.e., the torque/moment, which corresponds to the noncirculating flow of potential flow about the body, and difference to divide into normal force, then obtained thus the coordinate of center of pressure will correspond to purely circulation (viscous) flow. Let us call/name point with this coordinate the center of bound vortex. Let us designate the coordinate of the bound vortex

$$x_{\text{п}} = \frac{M_{z\text{эксп}} - M_{z\text{ин}}}{y_1}. \qquad (1)$$

Dimensionless coefficient of the center of the bound vortex

$$X_{\text{п}} = \frac{x_{\text{п}}}{b}.$$

In these formulas y_1 normal force; b is a root wing chord. As is known, in the adopted system the coordinates

$$M_{z\text{ин}} = -(r_2 - r_1)\frac{\rho V^2}{2}\sin 2\alpha,$$

where k_2 is a volume of the apparent additional mass of liquid during the motion of wing in transverse direction; k_1 - similar volume

during motion lengthwise. For the fine/thin wings $k_1 = 0$.

Page 25.

The experimental values of the center of bound vortex turn out to be considerably more stable in comparison with the center of pressure, which of low-aspect-ratio wings intensely moved to trailing edge with an increase in the angle of attack. The conclusion/derivation about the stability of the center of bound vortex finds confirmation, also, during the study of flow beyond wing. This gives grounds as the first basic hypothesis to consider that the position of the center of bound vortex for this wing planform does not depend on angle of attack.

The comparison of load distribution according to the wing chords of low elongation, designed according to linear theory and obtained experimentally, shows that during the determination of the position of the center of bound vortex it is possible to utilize values of the center-of-pressure coefficient and by the derivative of lift coefficient in root cross section, obtained in linear theory.

Then for a wing with symmetrical airfoil/profile, opening indeterminancy/uncertainty in the second term of expression (1), for a zero angle of attack we obtain

$$\overline{X}_{\text{п}} = C_{\text{д.т}} + \frac{\left(\frac{dm_{z\text{ин}}}{d\alpha}\right)_{\alpha=0}}{\left(\frac{dC_{yk}}{d\alpha}\right)_{\alpha=0}\frac{2rb}{s}},$$

where 2r - the spread/scope of the equivalent bound vortex of constant intensity.

As the second hypothesis for rectangular and elliptical in plan/layout wings let us assume that the spread/scope of bound vortex is equal the mean geometric spread/scope of wing, i.e.,

$$2r = \frac{s}{b}.$$

The experiments, carried out for determining the zone of eddying about the end/faces of wing, and also the spectra, obtained in water tunnel, confirm this assumption.

Further let us accept for low-aspect-ratio wings elliptical circulation distribution according to spread/scope, i.e., let us

set/assume

$$\left(\frac{dC_{yk}}{d\alpha}\right)_{\alpha=0} = \frac{4}{\pi}\left(\frac{dC_y}{d\alpha}\right)_{\alpha=0}.$$

Page 26.

Then we obtain working formula for determining the distance of the center of bound vortex from the leading edge:

$$\bar{X}_n = C_{д.л.т} + \frac{\left(\frac{dm_{zин}}{d\alpha}\right)_{\alpha=0}}{\frac{4}{\pi}\left(\frac{dC_{уп.т}}{d\alpha}\right)} C_{д.л.т} + \frac{2\frac{k_2}{sb}}{\frac{4}{\pi}\left(\frac{dC_{уп.т}}{d\alpha}\right)}.$$

The calculation methods, developed in S. M. Belotserkovskiy's book [1], make it possible to determine all values, entering this formula, for the case of motion near free interface at Froude's large

numbers, i.e., when on floating surface the disturbed speeds, parallel surfaces, will be equal to zero. Figure 1 gives the dependences of coefficients $X_{\text{п}}$ for a rectangular wing with $\lambda = 0.25$ on the value, reciprocal to relative insertion $\bar{h}=\frac{\eta}{l}$ (here η - the insertion of leading wing edge, l - the wingspan).

Figure 1 shows that with a decrease in the insertion of wing the center of bound vortex first is moved to leading wing edge, and then it begins to be moved to rear. This is explained by the fact that the coefficient of the center of pressure in linear theory barely depends on insertion; the moment derivative coefficient of inertia nature (it is expressed as the moment coefficient of inertia nature (it is expressed as the coefficient of the connected mass k_{21}) it falls with a decrease in the insertion, whereupon this incidence/drop at first very is intense, and subsequently moment coefficient is stabilized; the coefficient of derived lift falls with a decrease in the insertion, but this incidence/drop especially is intense of very interface. However practical value have the mainly descending legs of a curve $x_{\text{п}}(\frac{1}{\bar{h}})$, since with very low values $\bar{h}$ no longer is realized the nonseparated flow.

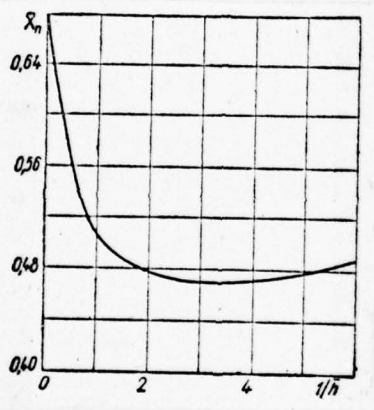

Fig. 1.

Page 27.

For the satisfaction of boundary condition about equality zero of caused speeds, parallel to the undisturbed surface, by taking into account in this case taper β free vortices, it is necessary to arrange higher than the interface the fictitious eddy/vortex, which is the representation of lower eddy/vortex relative to the undisturbed surface, as this is shown in Fig. 2.

The intensity of horse shoe vortex let us determine from the condition of the execution of chaplygina - Joukowski's postulate about the descent of jets under the rear point of root wing section. The caused at this point velocities must be determined not only from lower horse shoe vortex, but also from fictitious upper eddy/vortex.

In accordance with what has been said, it is above, is arranged rectangular low-aspect-ratio wing under floating surface so that when angle of attack is present, α leading wing edge has insertion η (Fig. 3). The lower bound vortex is arranged at a distance x_n from leading edge. Then the coordinates of point A for the coordinate system, connected with the upper bound vortex, will be

$$\bar{x}_D = \frac{\overline{CD}}{b} = \frac{(1 - x_n)\cos\alpha}{\cos\beta} - [\sin\alpha + 2\eta + x_n \sin\alpha + \\ + (1 - \bar{x}_n)\cos\alpha \operatorname{tg}\beta]\sin\beta; \qquad (2)$$
$$\bar{y}_D = \frac{\overline{AC}}{b} = -[\sin\alpha + 2\bar{\eta} + \bar{x}_n \sin\alpha + (1 - x_n)\cos\alpha \operatorname{tg}\beta]\cos\beta.$$

In formulas (2) of the line above x and η they designate, that these linear dimensions are referred to wing chord b. Cosine of angle DAE

$$\cos\delta = \frac{\bar{x}_D^2 + \bar{y}_D^2 + (1 - x_n)^2 - 4(\bar{\eta} + \bar{x}_n \sin\alpha)^2}{2\sqrt{\bar{x}_D^2 + \bar{y}_D^2}(1 - \bar{x}_n)}. \qquad (3)$$

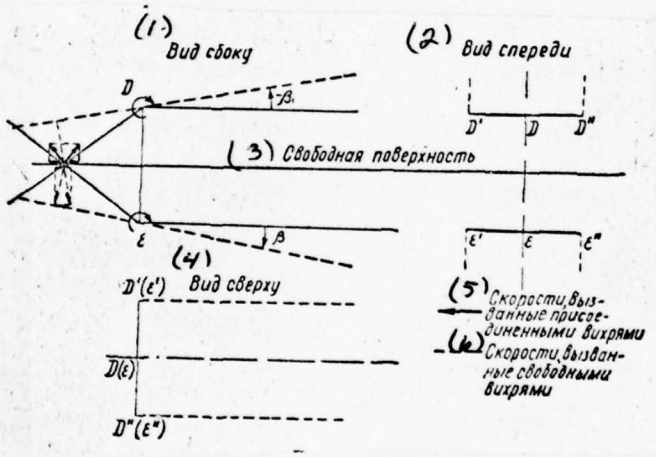
(1) Вид сбоку
(2) Вид спереди
D
D'
D
D"
(3) Свободная поверхность
ε'
ε
ε"
ε
(4) Вид сверху
D'(ε')
D(ε)
D"(ε")
(5) Скорости, вызванные присоединенными вихрями
(6) Скорости, вызванные свободными вихрями

Fig. 2.

Fig. 2.

Key: (1). Side view. (2). Front view. (3). Floating surface. (4). Plan view. (5). Velocities caused by bound vortexes. (6). Velocities caused by free vortices.

Page 28.

Velocity, caused at point A along the normal to chord by bound vortex D'D'',

$$(\omega_1)_D = \frac{\omega_{1D}}{v} = -\frac{C_{y0}}{4\pi} \frac{N_2 \cos\delta}{\sqrt{\bar{x}_D^2 + \bar{y}_D^2} \sqrt{\bar{x}_D^2 + y_D^2 + \left(\frac{\bar{\lambda}}{2}\right)^2}}, \quad (4)$$

where $C_{y_0} = \frac{2\Gamma}{vb}$ - the dimensionless coefficient of the intensity of horse shoe vortex.

Velocity, caused at point A along the normal to chord by the pair of free vortices, exiting/waste from bound vortex,

$$(\bar{w}_2)_D = \frac{w_{2D}}{v} = -\frac{C_{y_0}}{4\pi}\frac{N_2}{\bar{y}_D^2 + \left(\frac{\lambda}{2}\right)^2} \times$$

$$\times \left[1 + \frac{\bar{x}_D}{\sqrt{\bar{x}_D^2 + \bar{y}_D^2 + \left(\frac{\lambda}{2}\right)^2}}\right] \cos(\alpha + \beta). \qquad (5)$$

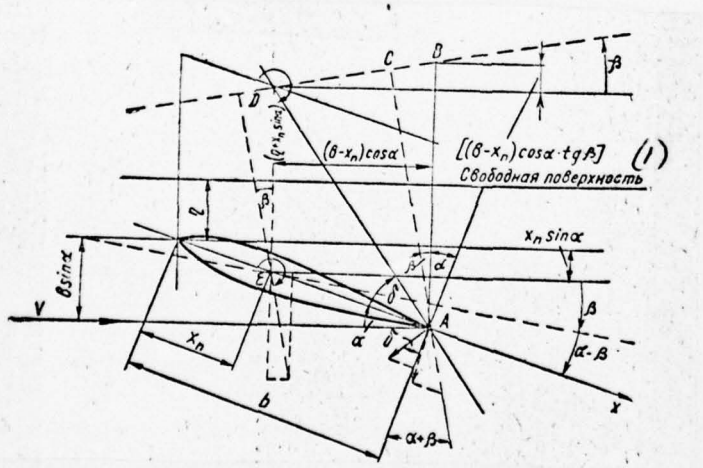

Fig. 3.

Key: (1) Floating surface.

The velocity, caused at point A along the normal to chord from bound vortex E'E'' and the pair of free vortices, exiting/waste from this bound vortex, will be

$$(\bar{w}_1)_E + (w_2) = -\frac{C_{y_0}}{4\pi}\left\{\frac{\lambda/2}{(1-x_n)\sqrt{(1-x_n)^2+\left(\frac{\lambda}{2}\right)^2}} + \right.$$

$$\left. + \frac{\frac{\lambda}{2}\cos(\alpha-\beta)}{(1-x_n)^2\sin^2(\alpha-\beta)+\left(\frac{\lambda}{2}\right)^2}\left[1+\frac{(1-x_n)\cos(\alpha-\beta)}{\sqrt{(1-\bar{x}_n)^2+\left(\frac{\lambda}{2}\right)^2}}\right]\right\}. \quad (6)$$

The dimensionless coefficient of the intensity of horse shoe vortex let us determine frcm the condition of the execution of chaplygina - Joukowski's postulate under point A of root wing section:

$$(\bar{w}_1)_D + (\bar{w}_2)_D + (\bar{w}_1)_E + (\bar{w}_2)_E + \sin\alpha = 0. \quad (7)$$

Hence

$$C_{u_0} = \frac{4\pi \sin\alpha}{\dfrac{\lambda/2}{(1-\bar{x}_n)\sqrt{(1-\bar{x}_n)^2+\left(\frac{\lambda}{2}\right)^2}} + \dfrac{\lambda/2\cos(\alpha-\beta)}{(1-x_n)^2\sin^2(\alpha-\beta)+\left(\frac{\lambda}{2}\right)^2}\times}$$

$$\times\left[1+\frac{(1-x_n)\cos(\alpha-\beta)}{\sqrt{(1-\bar{x}_n)^2+\left(\frac{\lambda}{2}\right)^2}}\right]+$$

$$+\frac{\lambda/2}{\sqrt{\bar{x}_D^2+\bar{y}_D^2}\sqrt{\bar{x}_D^2+\bar{y}_D^2+\left(\frac{\lambda}{2}\right)^2}}\cos\delta+$$

$$+\frac{\lambda/2}{\bar{y}_D^2+\left(\frac{\lambda}{2}\right)^2}\left[1+\frac{\bar{x}_D}{\sqrt{\bar{x}_D^2+\bar{y}_D^2+\left(\frac{\lambda}{2}\right)^2}}\right]\cos(\alpha+\beta) \qquad (8)$$

Downwash at points E' and E'' let us determine from the ratio of the vertical component of velocity v_y to the horizontal component of the velocity v_x in points E' or E''.

The velocity, induced with bound vortex D'D'', will be horizontal:

$$(w_{1x})_D = -\frac{C_{y_0}}{8\pi} \frac{\lambda}{2(\bar{\eta} + \bar{x}_n \sin\alpha)\sqrt{4(\bar{\eta} + \bar{x}_n \sin\alpha)^2 + \lambda^2}}. \quad (9)$$

two free vortices, exiting/waste from bound vortex D'D'', will give horizontal

$$(\bar{w}_{2x})_D = \frac{C_{y_0}}{8\pi} \frac{\lambda \sin\beta}{4(\bar{\eta} + \bar{x}_n + \sin\alpha)^2 \cos^2\beta + \lambda^2} \times$$
$$\times \left[1 - \frac{2(\bar{\eta} + \bar{x}_n \sin\alpha)\sin\beta}{\sqrt{4(\bar{\eta} + \bar{x}_n \sin\alpha)^2 + \lambda^2}} \right] \qquad (10)$$

and vertical the components of the velocity

$$(\bar{w}_{2y})_D = \frac{C_y}{8\pi} \frac{\lambda \cos\beta}{4(\bar{\eta} + \bar{x}_n \sin\alpha)^2 \cos^2 + \lambda^2} \times$$
$$\times \left[1 - \frac{2(\bar{\eta} + \bar{x}_n \sin\alpha)\sin\beta}{\sqrt{4(\bar{\eta} + \bar{x}_n \sin\alpha)^2 + \lambda^2}} \right]. \qquad (11)$$

Free vortex, exiting/waste from bound vortex at point E', will give the horizontal component of the velocity

$$(\bar{w}_{2x})_E = -\frac{C_{y_0}}{8\pi}\frac{\sin\beta}{\bar{\lambda}} \qquad (12)$$

and the vertical component of the velocity

$$(\bar{w}_{2y})_E = \frac{C_{y_0}}{8\pi}\frac{\cos\beta}{\bar{\lambda}}. \qquad (13)$$

By store/adding up vertical (11) and (13) and horizontal velocities of incident flow v at horizontal speeds (9), (10) and (12), we will obtain, taking into account smallness of angle β (tg β = sine β = β and cos β = 1),

$$\beta = \frac{V_y}{V_x} = \frac{\frac{C_{y_0}}{8\pi}\left\{\frac{\lambda}{4(\bar{\eta}+\bar{x}_n\sin\alpha)^2+\lambda^2}\times\right.}{1-\frac{C_{y_0}}{8\pi}\left\{\frac{\lambda}{2(\bar{\eta}+\bar{x}_n\sin\alpha)\sqrt{4(\bar{\eta}+\bar{x}_n\sin\alpha)^2+\lambda^2}}-\right.}$$
$$\times\left[1-\frac{2(\bar{\eta}+\bar{x}_n\sin\alpha)\beta}{\sqrt{4(\bar{\eta}+\bar{x}_n\sin\alpha)^2+\lambda^2}}\right]+\frac{1}{\lambda}\Bigg\}$$
$$-\frac{\lambda\beta}{4(\bar{\eta}+\bar{x}\sin\alpha)^2+\lambda^2}\times$$
$$\left.\times\left[1-\frac{2(\bar{\eta}+\bar{x}_n\sin\alpha)\beta}{\sqrt{4(\bar{\eta}+\bar{x}_n\sin\alpha)^2+\lambda^2}}\right]+\frac{\beta}{\lambda}\right\} \qquad (14)$$

Page 31.

The determination of the coefficient of the intensity of horse shoe vortex is conducted according to formulas (8) and (14) by consecutive propositions. For calculating coefficient C_{y_0} in the first approximation, is accepted the angle of the taper of free vortices β in zero approximation.

After determining C_{y_0} in the first approximation, they find, utilizing dependence (14), the angle of taper β in the first approximation,; on this rake angle from formula (8) is calculated the coefficient C_{y_1} the second approach/approximation etc.

Figure 4 and 5 depicts the results of the indicated calculations respectively from I to V approach/approximations for a wing with elongation λ = 0.25 and relative insertions $\bar{h}=\frac{\eta}{l}=1{,}7$ $(\bar{\eta}=\frac{\eta}{b}=\bar{h}\,\lambda=0{,}425)$.

From figures it is evident that for calculation C_{y_1} at angles of attack to 15° of third approach/approximation it is sufficient. At angle of attack into 25° it is required five approach/approximations.

As zero approximation for the angle of the taper of free vortices for the first calculation it is expedient to take β = 1/4 α,

and for the subsequent calculations - the values β, obtained for another (most close) insertion.

For determining the normal force, which acts on fine/thin wing, it is necessary to determine the longitudinal components of the velocities, induced by free vortices E' and E'', and also by horse shoe vortex D'D'' in the central cross section of bound vortex.

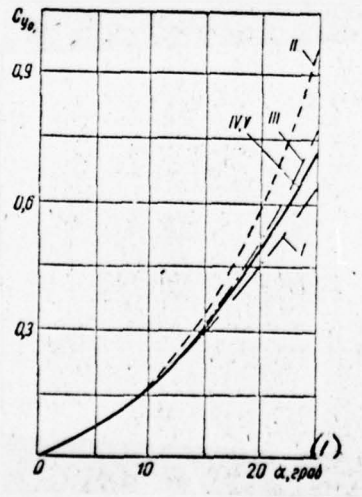

Fig. 4.

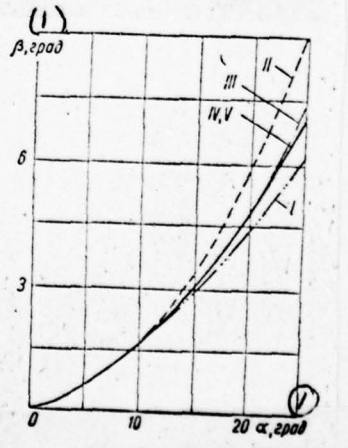

Fig. 5.

Fig. 4.

Key: (1). deg.

Fig. 5.

Key: (1). deg.

Page 32.

Velocity, induced by free vortices E' and E'' in the central cross section of bound vortex,

$$(\bar{w}_{2x_1})_E = \frac{C_{y_0}}{2\pi\lambda} \sin(\alpha - \beta). \qquad (15)$$

Further we compute the longitudinal component of the velocity, caused by bound vortex D:

$$(\bar{w}_{1x_1})_D = -\frac{C_{y_0} \cos\alpha\lambda}{16\pi(\bar{\eta} + \bar{x}_n \sin\alpha)\sqrt{4(\bar{\eta} + \bar{x}_n \sin\alpha)^2 + \left(\frac{\lambda}{2}\right)^2}}. \qquad (16)$$

Finally, the longitudinal component of the velocity, caused by free

vortices D' and D'',

$$(\overline{\omega}_{2x_1})_D = \frac{C_{y_1}\lambda}{8\pi} \frac{\sin(\alpha+\beta)}{4(\overline{\eta}+\overline{x}_n \sin\alpha)^2\cos^2\beta+\left(\frac{\lambda}{2}\right)^2} \times$$

$$\times \left[1 - \frac{2(\overline{\eta}+\overline{x}_n \sin\alpha)\sin\beta}{\sqrt{4(\overline{\eta}+\overline{x}_n \sin\alpha)^2+\left(\frac{\lambda}{2}\right)^2}}\right]. \qquad (17)$$

Taking into consideration that on the line of bound vortex E is a longitudinal component of dimensionless velocity of incident flow, equal cos α, applying the Joukowski theorum, we obtain this expression for the coefficient of the normal force of the fine/thin wing:

$$C_{y_1} = C_{y_1}[\cos\alpha + (w_{2x_1})_E + (\overline{w}_{1x_1})_D + (\overline{w}_{2x_1})_D]. \qquad (18)$$

For fine/thin wings as a result of flow breakaway on leading

edge the suction force is not realized, and, design/projecting the coefficient of normal force for drag axes, we will obtain for the lift

$$C_y = C_{y_1} \cos \alpha \qquad (19)$$

and for the coefficient of an increase in the resistance, caused by the presence of angles of attack,

$$C_x - C_{x_0} = C_{y_1} \sin \alpha. \qquad (20)$$

Page 33.

The coefficient of the longitudinal moment with respect to leading edge is equal to the sum of the moment coefficients of vortex/eddy nature and torque/moment of inertia nature and of the adopted by Fig. 3 system of coordinates is record/written in the form

$$m_z = m_{z\delta} + m_{z\text{ин}} = C_{y_1} \bar{x}_n - \frac{k_2}{sb} \sin 2\alpha. \qquad (21)$$

Finally, the dimensionless coordinate of center of pressure

$$C_{\text{д}} = \frac{x_{\text{д}}}{b} = \frac{m_z}{C_{y_1}} = \bar{x}_{\text{д}} - \frac{k_2}{sb}\frac{\sin 2\alpha}{C_{y_1}}. \qquad (22)$$

Figure 6-8 gives the results of the calculations of the lift coefficients, coefficients of an increase in resistance and center-of-pressure coefficients of fine/thin wing with elongation λ = 0.25 with several relative insertions.

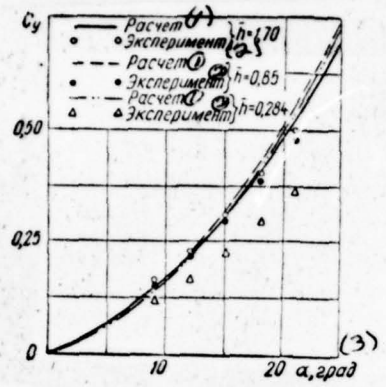

Fig. 6.

Key: (1). Calculation. (2). Experiment. (3). deg.

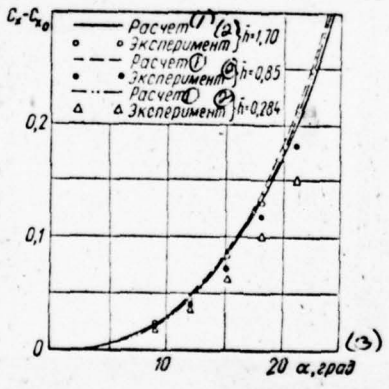

Fig. 7.

Key: (1). Calculation. (2). Experiment. (3). deg.

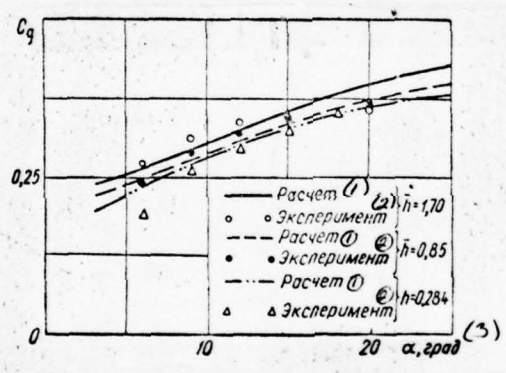

Fig. 8.

Key: (1) Calculation; (2) Experiment; (3) deg.

Page 34.

Theoretical curves for very small relative insertion h = 0.284 lie/rest above experimental points, that it is possible to explain by the presence during this insertion of flow with filled by air by vortex lines.

The essential nonlinearity of moment coefficient leads to the fact that the center of pressure sufficiently intensely moved to trailing wing edge with an increase of angle of attack.

It is interesting to note that a decrease in the relative insertion in the en. of time, virtually without changing lift coefficients, noticeably manifests itself the center-of-pressure location. With a decrease in the relative insertion the center of pressure is moved to leading edge, which also is confirmed by experiment.

Bibliography

1. Белоцерковский С. М. Тонкая несущая поверхность в дозвуковом потоке газа. «Наука», М., 1965.
2. Федяевский К. К., Соболев В. Г. Управляемость корабля, Судпромгиз, Л., 1963.

WAVE LOAD ON THE VERTICAL WING OF MAXIMALLY LOW ELONGATION.

G. V. Sobolyev.

(Leningrad).

On the basis of common/general/total theory, presented in monograph [3], it is possible to manufacture the calculations of the different of the shape of the lifting surfaces, which work on the interface of different density. For the case of the vertical wing in this work is also obtained the integral equation of circulation distribution in the prerequisite/premises of the supporting line, which is justified for the wings of the average and great lengthenings. With the smallness of lengthening it is necessary to assume the unknown load of variable both chordwise and in spread/scope. In this case the task becomes mathematically very complex. In this article is made the attempt to bring the unpacking/facings of solution to end in the extreme case of the wing of very low lengthening.

We have obtained integrodifferential equation for the

distribution of the transverse load, appearing during motion near the floating surface of vertical fine/thin wing. The case, when the chord of fine/thin wing coincides with the undisturbed surface of liquid and its relation to spread/scope l is great (i.e. wing aspect ratio $\bar{l}=\frac{b}{l}\to 0$), is especially interesting for ship-builders. This hypothetical case can be used as schematic for the calculation of load on shipboard housing so on its motion with drift angle β. In the general case of curvilinear motion this angle will be variable along the length $\beta(x)$.

Integrodifferential equation of the relatively dimensionless coefficient of pressure u (x, z), obtained with the assumptions, common for the linear theory of waves and airfoil theory

$$\beta(x)=\frac{1}{2\pi}\int_{-l/2}^{l}\int_{0}^{0}\frac{du(\xi,\zeta)}{d\zeta}\left[\frac{1}{z-\zeta}+\frac{1}{z+\zeta}+K(x,\xi,z,\zeta)\right]d\zeta d\xi, \quad (1)$$

where

$$K(x,\xi,z,\zeta)=\frac{4}{\pi F^2}\int_{1}^{\infty}\sqrt{1-\frac{1}{t}}\cos\left[\frac{(x-\xi)\sqrt{t}}{F^2}\right]\exp\frac{t(z+\zeta)}{F^2}dt.$$

The relative velocity $F = \frac{v}{\sqrt{gb}}$ and all coordinates are referred in this expression to the chord length of wing - b, but the position of beginning and the direction of axle/axes is shown in Fig. 1.

To first two terms in equation (1) it is logical to shape in the form, similar to the case of the motion of wing near solid screen. In this case they can be united into one member with the symmetrical limits of integration on ζ:

$$\beta(x) = \frac{1}{2\pi}\int_{1/2}^{x}\int_{-l}^{l}\frac{1}{z-\zeta}\frac{du(\xi,\zeta)}{d\zeta}\,d\zeta d\xi + \frac{1}{2\pi}\int_{1/2}^{x}\int_{-l}^{0}K(x,\xi,z,\zeta)\times$$
$$\times\frac{du(\xi,\zeta)}{d\zeta}\,d\zeta d\xi. \qquad (2)$$

This recording, of course, introduces the inaccuracy, which consists under the assumption of the symmetry of distribution u (z) in real and mirror reflected relative to floating surface planes. However, if we restrict the examination by the case of the small numbers Fr, then the proximity of the unknown load distribution to limiting case Fr $\rightarrow$ 0, by which it elliptical, can be considered obvious.

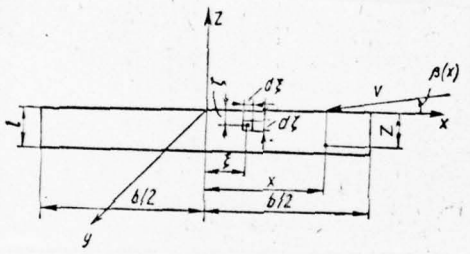

Fig. 1.

Equality (2) is integral equation of Volterra's type relative to the function, which determines the character of the dependence of load along the length of chord. The law of span loading depends in essence on singular term in the first integral. For the

isolation/liberation of this special feature/peculiarity let us manufacture the regularization of equation (2) for Carleman-Wekua's method [3].

Let us transpose regular wave member into the left side and for the moment that consider this part assigned. Then let us manufacture the inversion of Cauchy integral in right side relative to function $\int_{1/2}^{x} \frac{du(\xi\zeta)}{d\zeta} d\xi$.

Solution let us search for in the broadest class of the functions, unconfined at the ends of the interval/gap of integration on ζ:

$$\int_{1/2}^{x} \frac{du(\xi, \zeta)}{dz} d\xi = -\frac{1}{\pi \sqrt{l^2 - z^2}} \left[2\beta(x) \int_{-l}^{l} \frac{\sqrt{l^2 - \tau^2}}{\tau - z} d\tau + \right.$$

$$\left. + \int_{-l}^{l} \int_{1/2}^{x} \int_{-l}^{0} \frac{du(\xi, \zeta)}{d\zeta} \frac{\sqrt{l^2 - \tau^2}}{\tau - z} K(x, \xi, \tau, \zeta) \, dz d\xi d\tau + f(x) \right]. \quad (3)$$

The entering the inversion formula arbitrary constant, in the case in question which is the function of the longitudinal coordinate f (x),

subsequently must be determined from the condition of the satisfaction of solution Chaplygin-to Jcukcwski's postulate. For the calculation of integrals in terms of auxiliary variable τ let us introduce the trigonometric coordinates

$$z = -l\cos\theta;\ \zeta = -l\cos\vartheta \text{ и } \tau = -l\cos\varphi,$$

we will obtain

$$\int_{\pi/2}^{x} \frac{du(\xi, \theta)}{d\theta} d\xi = 2\beta(x) l \int_{0}^{\pi} \frac{\sin^2\varphi d\varphi}{\cos\varphi - \cos\theta} +$$
$$+ l \int_{0}^{\pi} \int_{\pi/2}^{x} \int_{0}^{\pi/2} \frac{du(\xi, \vartheta)}{d\vartheta} \frac{\sin^2\varphi k(x, \xi, \varphi, \vartheta)}{\cos\varphi - \cos\theta} d\vartheta d\xi d\varphi. \qquad (4)$$

The being obtained here integrals take the form

$$B = \int_0^{\pi} \frac{\sin^2 \varphi \exp - b \cos \varphi}{\cos \varphi - \cos \theta} d\varphi, \qquad (5)$$

where b = 0 for first integral in right side and b = $\frac{tl}{F^2} = \frac{t}{F_i^2}$ for the second integral.

Page 38.

Let us note that on the strength of the evenness of integrand in (5) value B can be calculated as half of integral with the symmetrical limits:—π-π. Now let us introduce new alternating/variable $z = e^{i\varphi}$, transforming B into contour integral of complex variable z:

$$B = \mathrm{Re} \left| \frac{1}{4i} \oint \frac{(z^2 - 1)^2 \exp - \frac{b}{2z} (z^2 + 1)}{z^2 (z^2 - 2z \cos \theta + 1)} dz \right|.$$

Since coefficient b it is always positive value, singular point

from member $e^{\frac{1}{z}}$ it is not obtained and for calculation B necessary to obtain the deductions of the function

$$f(z) = \frac{(z^2 - 1)\exp - \frac{b}{2x}(z^2 + 1)}{z^2(z^2 - 2z\cos\theta + 1)}$$

in the twofold pole z = 0 and at the points

$$z_i = \cos\theta \pm i\sin\theta \quad (i = 1, 2),$$

being the roots of the equation

$$z^2 - 2z\cos\theta + 1 = 0.$$

The first special feature/peculiarity it gives zero deduction because of member $e^{-\frac{b}{2z}(z^2+1)}$ which in the case of conjugate roots z_i it takes form exp - b cos θ.

Therefore

$$B = \mathrm{Re}\left|2\pi i \frac{1}{4i}\,\mathrm{Res} f(z)\right| = \frac{\pi}{4}\, e^{-b\cos\theta}\,\mathrm{Re}\left|\sum_{i=1}^{2} \frac{(z_i^2 - 1)^2}{2z_i^3 - 3\cos\theta z_i^2 + z_i}\right|.$$

After the substitution of values z_i and of separation on real and imaginary part we obtain

$$B = -\pi \cos\theta \exp - b\cos\theta. \tag{6}$$

Taking into account value (6) equation (4) assumes the form

$$\int_{1/2}^{x} \frac{du(\xi,\theta)}{d\theta}\,d\xi = -2\beta(x)\,l\cos\theta - \frac{4}{\pi F_l^2}\cos\theta \int_0^{\pi/2}\int_0^{x} \frac{du(\xi,\vartheta)}{d\vartheta} \times$$
$$\times \int_1^{\infty} \sqrt{1-\frac{1}{t}}\cos\frac{(x-\xi)\sqrt{t}}{F^2}\exp -\frac{t}{F_l^2}(\cos\vartheta+\cos\theta)\,dt\,d\xi\,d\vartheta + f(x). \tag{7}$$

Page 39.

Let us take in parts integral of ϑ, taking into account that u (ξ, ϑ) must be equal to zero as at the butt end of the wing, that and on floating surface. By making, furthermore, integration for ϑ, let us return in equation (7) to primitive function u:

$$\int_{1/2}^{x} u(\xi, \theta)\, d\xi = -2\beta(x)\, l \sin\theta + \frac{4}{\pi F_l^2} \int_{1/2}^{x}\int_{0}^{\theta} \cos\varphi \int_{0}^{\pi/2} u(\xi, \vartheta) \sin\vartheta \times$$

$$\times \int_{1}^{\infty} \sqrt{t^2 - t}\, \cos\frac{(x-\zeta)\sqrt{t}}{F^2} \exp -\frac{t}{F_l^2} (\cos\vartheta + \cos\varphi)\, dt d\vartheta d\xi + f(x). \tag{8}$$

For determining the character of load distribution chordwise of wing let us pass from specific pressure to load per unit of length $\gamma(x)$:

$$\gamma(x) = \int_{-l}^{0} u(\xi, z)\, dz = l \int_{0}^{\pi/2} u(\xi, \theta) \sin\theta\, d\theta.$$

Then equation (8) is written as follows:

$$\int_{l/2}^{x} \gamma(\xi)\, d\xi = -2\beta(x)\, l^2 \int_0^{\pi/2} \sin^2\theta\, d\theta +$$

$$+\frac{4l}{\pi F_l^2} \int_{l/2}^{x} \int_0^{\pi/2} \sin\theta \int_0^{\theta} \cos\varphi \int_0^{\pi/2} u(\xi, \vartheta) \sin\vartheta \int_1^{\infty} \sqrt{t^2-t}\, \cos\frac{(x-\xi)\sqrt{t}}{F^2} \times$$

$$\times \exp -\frac{t}{F_l^2}(\cos\vartheta + \cos\varphi)\, dt d\vartheta d\varphi d\theta d\xi + f_1(x). \qquad (9)$$

Let us assume now that the unknown function of load distribution u (x, θ) can be represented in the form of the product

$$u(x, \theta) = \gamma(x)\, z(\theta). \qquad (10)$$

Physically this it means that the law of span loading is assumed to be one and the same in all cross sections of wing chord. Recall that the load on the wing of maximally low lengthening in infinite liquid is sharply localized on the spout of wing. Examine/considered

by us the case of the moderate velocities of motion on interface must be close to this maximum.

Page 40.

Therefore relationship/ratio (10) is completely justified. Taking into account it in (9), we have

$$\int_{l/2}^{x} \gamma(\xi)\, d\xi = -\frac{\pi}{2}\beta(x)\, l^2 + \int_{l/2}^{x} \gamma(\xi)\, k(x, \xi)\, d\xi + f_1(x), \qquad (11)$$

where

$$k(x, \xi) = \frac{4l}{\pi F_l^2} \int_0^{\pi/2} \sin\theta \int_0^{\theta} \cos\varphi \int_0^{\pi/2} z(\vartheta) \sin\vartheta \int_1^{\infty} \sqrt{t^2 - t} \cos\frac{(x-\xi)\sqrt{t}}{F^2} \times$$

$$\times \exp -\frac{t}{F_l^2}(\cos\vartheta + \cos\varphi)\, dt d\vartheta d\varphi d\theta. \qquad (12)$$

Differentiating (11) with respect to x, we obtain

$$\gamma(x) = -\frac{d}{dx}\left[\frac{\pi}{2}\beta(x)l^2\right] + \gamma(x)\,k(x, x) + \int_{1/2}^{x} \gamma(\xi)\frac{dk(x, \xi)}{dx}\,d\xi.$$

easy to see, that the first member in right side coincides with that which was obtained by us by solution [4] for case Fr = 0:

$$\gamma_0(x) = -\frac{\pi}{2}\frac{d}{dx}[\beta(x)\,l^2(x)]. \qquad (13)$$

Value

$$k(x, x) = \frac{4l}{\pi F_l^2}\int_0^{\pi/2}\sin\theta\int_0^{\eta}\cos\varphi\int_0^{\pi/2}z(\vartheta)\sin\vartheta\int_1^{\infty}\sqrt{t^2-t}\exp-$$
$$-\frac{t}{F_l^2}(\cos\vartheta+\cos\varphi)\,dt\,d\vartheta\,d\varphi\,d\theta$$

is the solidity ratio of the diagram/curve of the distribution of wave load according to spread/scope (sinking)

$$-k(x, x) = \alpha = f(F).$$

Designating kernel of integral equation F (x, ξ) = dk (x, ξ) /dx, we have

$$\gamma(x)(1+\alpha) = \gamma_0(x) + \int_{1/2}^{x} \gamma(\xi) F(x, \xi)\, d\xi + f_2(x). \qquad (14)$$

Let us note that the entering the expression α integral

$$D = \int_{1}^{\infty} \sqrt{t^2 - t}\, \exp - dtdt,$$

where

$$d = (\cos\vartheta + \cos\varphi)\frac{1}{F_i^2}$$

is tabular (see [2] 3.383 (3)):

$$D = \frac{k_1\left(\frac{d}{2}\right)\exp -\frac{d}{2}}{2d}$$

(k_1 (d/2) - the function of Macdonald).

Page 41.

Taking into account this value in α, we have

$$\alpha = -\frac{2l}{\pi}\int_0^{\pi/2} \sin\theta \int_0^{\theta} \cos\varphi \int_0^{\pi/2} z(\vartheta)\sin\vartheta \times$$

$$\times \frac{k_1\left(\frac{\cos\vartheta + \cos\varphi}{2F_i^2}\right)\exp -\left(\frac{\cos\vartheta + \cos\varphi}{2F_i^2}\right)}{\cos\vartheta + \cos\varphi} d\vartheta d\varphi d\theta. \qquad (15)$$

Since $F_l^2 = \frac{v}{gbb/l} = \frac{F^2}{l}$ with $l \to 0$ very greatly, let us replace the value of the function of the Macdonald and exponential for asymptotic. For this is expressed k_1 (d/2) through the degenerate hypergeometric function $\Psi(a, c, x)$, the character of behavior of which with low x is known.

Since

$$k_\nu(x) = \sqrt{\pi} e^{-x} (2x)^\nu \Psi\left(\frac{1}{2} + \nu;\ 1 + 2\nu;\ 2x\right),$$

$$k_1\left(\frac{d}{2}\right) = \sqrt{\pi} e^{-d/2} d\Psi(3/2;\ 3;\ d). \qquad (16)$$

With low d we have

$$\Psi(a, c, x) = x^{1-c} \frac{\Gamma(c-1)}{\Gamma(a)}$$

with an accuracy down to the terms with /x/. This it gives

$$\Psi\left(\frac{3}{2};\ 3;\ d\right)=\frac{1}{d^2}\frac{2}{\sqrt{\pi}}+|d|. \qquad (17)$$

Taking into account (16) and (17), we obtain

$$\alpha=-\frac{4F^2}{\pi}\int_0^{\pi/2}\sin\theta\int_0^{\theta}\cos\varphi\int_0^{\pi/2}z(\vartheta)\sin\vartheta\,\frac{d\vartheta}{(\cos\vartheta+\cos\varphi)^2}\,d\varphi d\theta. \qquad (18)$$

Page 42.

After changing in this expression the order of the integration:

$$\alpha=-\frac{4F^2}{\pi}\int_0^{\pi/2}z(\vartheta)\sin\vartheta\int_0^{\pi/2}\sin\theta\int_0^{\theta}\frac{\cos\varphi d\varphi}{(\cos\vartheta+\cos\varphi)^2}\,d\theta d\vartheta,$$

let us compute integrals in terms of ϕ and θ, by reject/throwing terms with the low values:

$$a = -\frac{4F^2}{\pi}\int_0^{\pi/2} \frac{z(\vartheta)\cos\vartheta}{\sin\vartheta,} \ln\cos\vartheta d\vartheta. \qquad (19)$$

Accepting as first approximation z (ϑ) = sine ϑ, we obtain

$$a = -\frac{4F^2}{\pi}\int_0^{\pi/2} z(\vartheta)\cos\vartheta \ln\cos\vartheta d\vartheta =$$

$$= \frac{F^2}{\pi} B\left(\frac{1}{2};\ 1\right)\left[\Psi\left(\frac{3}{2}\right) - \Psi\left(\frac{1}{2}\right)\right]$$

(see [2] 4.387 (1)). Taking into account the value of β-function B (1/2; 1) and difference Ψ - Euler functions $\Psi\left(\frac{3}{2}\right) - \Psi\left(\frac{1}{2}\right)$, we have the final value of solidity ratio of wave load diagram on the wing of the

maximally low lengthening:

$$a = \frac{2F^2}{\pi}. \tag{20}$$

I investigate now the character of load distribution chordwise, described by equation (14). Investigating the integral

$$C = \int_1^\infty \sqrt{t^2 - t}\, \exp - td \cos a\sqrt{t}\, dt, \tag{21}$$

where

$$a = \frac{x - \xi}{F^2},$$

we will obtain expression F (x, ξ) in an explicit form. Expanding cos $a\sqrt{t}$ in power series, we have

$$C = \int_1^{\infty} \sqrt{t^2 - t} \exp -td \left(1 - \frac{a^2}{2!} t + \frac{a^4}{4!} t^2 - \ldots\right) dt.$$

Page 43.

Assuming, that termwise integration it does not disturb the convergence of this series, we obtain

$$C = -\frac{\sqrt{\pi}}{2} e^{-d/2} \sum_{n=0}^{\infty} (-1)^n \frac{a^{2n}}{2n!} d^{-\frac{n+3}{2}} W_{\frac{n}{2}, -\frac{n+2}{2}}(\alpha)$$

(see [2] 3.383 (4)). Expressing Whittaker function $W_{\frac{n}{2}, -\frac{n+2}{2}}(\alpha)$ through the degenerate hypergeometric function $\Psi\left(a; c; \frac{2}{x}\right)$

$$W_{\varkappa,\mu}(x) = e^{-x/2}\, x^{c/2}\, \Psi(a;\ c;\ x);$$

$$a = \frac{1}{2} - \varkappa + \mu;$$

$$c = 2\mu + 1,$$

we obtain

$$C = \frac{\sqrt{\pi}}{2}\, e^{-d} \sum_{n=0}^{\infty} (-1)^n \frac{a^{2n}}{2n!}\, \Psi\left(\frac{3}{2},\ n+3, d\right). \qquad (22)$$

Replacing, as earlier, expression Ψ by its asymptotic value with $d \to 0$, in which it makes sense to leave the terms not higher than second order of smallness, we have

$$C = -e^{-a}\frac{1}{d^2}\sum_{n=0}^{\infty}(-1)^n\frac{a^{2n}}{2n!}\,n! \approx$$

$$\approx -\frac{e^{-a}}{d^2}\sum_{n=0}^{\infty}(-1)^n\frac{a^{2n}}{(2n)!!\,(2n)!!} = -\frac{e^{-a}}{a^2}J_0(a), \qquad (23)$$

where J_0 (a) - the Bessel function of zero-order.

Taking into account these conversions equation (14) will be written as follows:

$$\gamma(x) = \frac{1}{1+a}\gamma_0(x) - \frac{2}{\pi(1+a)}\int_{l/2}^{x}\gamma(\xi)\,J_1\left(\frac{x-\xi}{F^2}\right)d\xi + f_2(x). \qquad (24)$$

As is known from the theory of integral equations of Volterra's type,

solution (24) can be written in the form of the series

$$\gamma(x) = \sum_{n=0}^{\infty} \left(\frac{2}{\pi}\right)^n \frac{\gamma_n(x)}{(1+\alpha)^{n+1}}. \qquad (25)$$

where

$$\gamma_{n+1}(x) = \int_{1/2}^{x} J_0\left(\frac{x-\xi}{F^2}\right) \gamma_n(\xi)\, d\xi. \qquad (26)$$

Page 44.

We will be restricted to the search of the first term of this series, which will correspond to the solution, obtained with an accuracy down to the terms with F^4.

Taking into account value $\gamma_0(x)$, according to formula (13), we obtain

$$\gamma_1(x) = -\frac{\pi}{2}\int_{1/2}^{x} J_1\left(\frac{x-\xi}{F^2}\right)\frac{d}{d\xi}[l^2(\xi)\,\beta(\xi)]\,d\xi. \qquad (27)$$

For right-angled wing

$$\gamma_1(x) = -\frac{\pi l^2}{2}\int_{1/2}^{x} J_1\left(\frac{x-\xi}{F^2}\right)\frac{d\beta(\xi)}{d\xi}\,d\xi.$$

During the forward motion of wing $\beta(\xi) = \text{const} = \beta_0$ and $d\beta(\xi)/d\xi = 0$ everywhere, besides forepart/nose edge ($x = 0.5$), where $d\beta(\xi)/d\xi = -\beta_0$. Then

$$\gamma_1^{\beta}(x) = -\frac{\pi l^2}{2} J_1\left(\frac{0,5-x}{F^2}\right). \qquad (28)$$

It is easy to see, that solution (28) in the general case it does not

satisfy Chaplygin-Joukowski's hypothesis about the even flow of tail edge. In order that this hypothesis is fulfilled, it is necessary that load with x = -0.5 is absent. Determining until now the arbitrary function f_2 (x), that entered in equation (24), finally we obtain

$$\gamma_1^{\beta}(x) = \frac{\pi l^2}{2}\left[J_1\left(\frac{0,5-x}{F^2}\right) - J_1\left(\frac{1}{F^2}\right)\right]. \qquad (29)$$

Curve/graph of the distribution of this wave load for a series of the values of relative velocity is shown in Fig. 2.

By analyzing curves, it is possible to note that to Fr = 0.6-0.65 transverse loads from waves gives positive additions to the hoisting (lateral) force of the wing of maximally low lengthening. The maximum of this increase is reached when on wing chord is accomodated one half wave (Fr $\approx$ 0.5). At such relative velocities one should expect the maximum effect of floating surface. With an increase of velocity together with a decrease in the number of waves, which are placed on chord, proceeds the shift/shear of the first (most considerable) peak of pressures from spout toward tail edge.

This fact makes it possible to state/establish an increase dream the weathercock stability of wings, which is really/actually observed in experiments.

Unfortunately, the calculation of the lift coefficients of the wing

$$C_y = \frac{2}{l}\int_{-0.5}^{0.5} \gamma(x)\,dx \qquad (30)$$

and of the torque/moment

$$m_z = \frac{2}{l}\int_{-0.5}^{0.5} \gamma(x)\,x\,dx \qquad (31)$$

in expressions (25), (13) and (29) cannot be made in quadratures. however the measuring with planimeter of the curves of Fig. 2 and the calculations they show that an increase in the coefficient C_y is

observed to Pr = 0.6. Subsequently value of C_v becomes virtually independent variable of velocity and is equal to the value, designed by the formulas of infinite liquid without taking into account of the screening effect of floating surface.

That which was opened thus far remains the question concerning convergence of series (25), coefficients $\left(\frac{2}{\pi}\right)^n \frac{1}{(1+\alpha)^{n+1}}$ which they decrease sufficiently slowly.

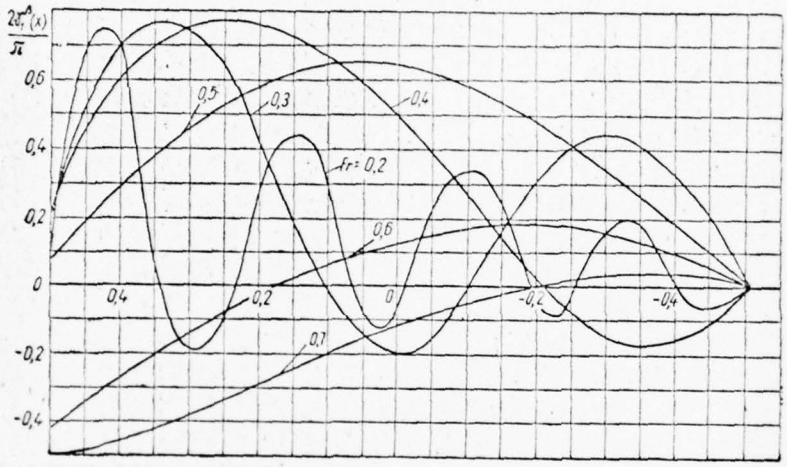

Fig. 2.

Page 46.

Bibliography.

1. Гахов Ф. Д. Краевые задачи. Физматгиз, М., 1963.
2. Градштейн И. С., Рыжик И. М. Таблицы интегралов. Физматгиз, М., 1963.
3. Панченков А. Н. Гидродинамика подводного крыла. «Наукова думка», К., 1965.
4. Федяевский К. К., Соболев Г. В. Управляемость корабля. Судпромгиз, Л., 1963.

CAVITATION FLOW ABOUT THE WEDGE NEAR THE FLOATING SURFACE OF WEIGHTLESS LIQUID.

L. I. Maltsev.

(Novosibirsk).

Page 56.

It is known that during the motion of body in nonseparable and cavitation mode/conditions the large value for a reduction/descent in the resistance has pressure recovery in its feed part. However, in the works, dedicated to the cavitating hydrofoils, as a rule, floating surfaces, being broken away from edges, are linked somewhere beyond the limits of body or depart to infinity. The quality of such wings turns out to be low. Is examined below the simplest diagram of the cavitating hydrofoil, which ensures the pressure recovery aft.

The solution of this problem for a unrestricted flow is obtained in work [5]. The advisability of the examination of the partially cavitating wings was expressed by B. G. Novikov.

Let us examine the task of the cavitation flow about the wedge near the floating surface of weightless liquid.

By v_∞, v_0, l_1, l_2, τ, μ let us designate respectively velocity of incident flow, rate on the boundary/interface of cavern, the length of plates OB and OC, angle between them and the angle of the slope of plate to direction, the opposite direction of the incident flow (Fig. 1).

The flow line, which approaches the critical point A, is located from floating surface far from wedge at a distance H. It is assumed that the point O is the point of the descent of jets, i.e., that is satisfied chaplygina - Joukowski's condition.

In the physical plane let us conduct the cut/section through point O and certain point on floating surface.

Page 57.

The obtained thus simply connected region is resolvable to the interior of rectangle with sides $2\omega_1$, ω_2 the auxiliary plane u, so as to the shores of cut/section will pass to the vertical sides of rectangle (Fig. 2). The appropriate points let us designate by identical letters.

Let us introduce the function

$$F = \ln\left(\frac{1}{v_\infty}\frac{dW}{dz}\right) = \ln\frac{v}{v_\infty} - i\vartheta = p - iq \left(\frac{dW}{dz} = ve^{-i\vartheta}\right).$$

It is known that the solution of problem can be reduced to the determination of the dependences

$$W(u) \text{ и } F(u).$$

Let us determine function $\frac{\partial W}{\partial u}$ [2]. Function dW/du is holomorphic within rectangle, is real on its horizontal sides, and its values on the vertical sides of rectangle at the corresponding points coincide. The continued through the sides of rectangle function dW/du will be bioperiodic. Furthermore, at points u = α and u = 0 dW/du it must have zeros, but at point δ + ω_2 - the pole of the second order.

Hence it follows that dW/du there is an elliptical function. On the basis of the common/general/total theory of the elliptical functions

$$\frac{dW}{du} = A[\wp(u-\delta-\omega_2)-\wp(a-\delta-\omega_2)]. \qquad (1)$$

where A is real constant.

The requirement for reduction to zero rate at point 0 (u = 0) gives the condition

$$a = 2\delta. \qquad (2)$$

By set/assuming complex potential equal to zero at point A, for W (u) we will obtain the expression

$$W(u) = -A[\zeta(u-\delta-\omega_2)-\zeta(\delta-\omega_2)+\wp(\delta-\omega_2)(u-2\delta)]. \quad (3)$$

Page 58.

Circulation on the closed duct, which covers wing,

$$\Gamma = W(2\omega_1)-W(0) = -2A[\zeta(\omega_1)+\wp(\delta-\omega_2)\omega_1]. \qquad (4)$$

Utilizing the fact that

$$W(u_1+\omega_2)-W(u_1) = Hv_\infty,$$

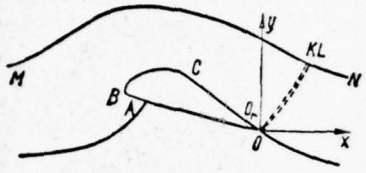

Fig. 1.

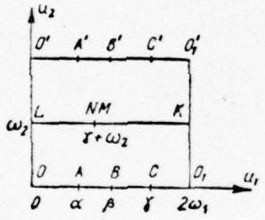

Fig. 2.

we will obtain

$$H = \frac{\pi A - i\omega_2 \Gamma}{2\omega_1 \bar{v}_\infty}. \tag{5}$$

Let us pass to the determination of function F (u). Function F (u) on the horizontal sides of rectangle satisfies the boundary condition

$$\begin{aligned}
&q = -\mu && (0 < u_1 < \alpha);\\
&q = \pi - \mu && (\alpha < u_1 \leqslant \beta);\\
&q = -\tau && (\gamma \leqslant u_1 < 2\omega_1);\\
&p = \ln \frac{v_0}{v_\infty} && (\beta \leqslant u_1 \leqslant \gamma) \text{ with } u = u_1;\\
&p = 0 \text{ with } && u = u_1 + \omega_2.
\end{aligned}$$

The solution to the obtained mixed boundary-value problem for the rectangle, limited near all ends, we will obtain from L. I. Sedov's method [3]:

$$F(u) = \frac{1}{x_i}\left[\ln\frac{v_0}{v_\infty}\int_\beta^\gamma g(u_1 t)\,dt + i\mu\int_0^\alpha g(u_1 t)\,dt - i(\pi-\mu)\int_\alpha^\beta g\times\right.$$
$$\left.\times(u_1 t)\,dt + i\tau\int_\gamma^{2\omega_1} g(u_1 t)\,dt\right];$$
$$g(u_1 t) = e^{\eta_1(t-u)}\,\frac{\sigma(u-t+c)\,\sigma^2(t-\delta-\omega_2)\,\sigma(u-\omega_2)}{\sigma(c)\,\sigma(u-t)\,\sigma^2(u-\delta-\omega_2)\,\sigma(t-\omega_2)}\times$$
$$\times\sqrt{\frac{\sigma(u-\beta)\,\sigma(u-\gamma)}{\sigma(t-\beta)\,\sigma(t-\gamma)}}, \qquad (6)$$

where σ (u) - Weierstrass function;

$$c = \omega_1 - \alpha + \frac{\beta + \gamma}{2} - \omega_2; \qquad \eta_1 = \zeta(\omega_1).$$

Page 59.

In order that the solution becomes zero at the point $\delta + \omega_2$, corresponding to point at infinity of the physical plane, necessary to require satisfaction of the conditions

$$i \ln \frac{v_0}{v_\infty} \int_\beta^\gamma g_\kappa(t)\, dt + \mu \int_\delta^\alpha g_\kappa(t)\, dt - (\varkappa - \mu) \int_\alpha^\beta g_\kappa(t)\, dt + \\ + \tau \int_\gamma^{2\omega_1} g_\kappa(t)\, dt = 0 \qquad (k = 1, 2, 3). \tag{7}$$

where

$$g_1(t) = e^{\eta_1 t}\,\frac{\sigma(\Delta + t)\,\sigma(-t + \delta + \omega_2)}{\sigma(t - \omega_2)\sqrt{\sigma(t-\beta)\,\sigma(t-\gamma)}};$$

$$g_2(t) = e^{\eta_1 t}\left[\frac{\sigma'(\Delta - t)\,\sigma(-t + \delta + \omega_2) - \sigma(\Delta - t)\,\sigma'(-t + \delta + \omega_2)}{\sigma(t - \omega_2)\sqrt{\sigma(t-\beta)\,\sigma(t-\gamma)}}\right];$$

$$g_3(t) = e^{\eta_1 t}\left\{\frac{\sigma''(\Delta - t)\,\sigma(-t + \delta + \omega_2) - \sigma(\Delta - t)\,\sigma''(-t+\delta+\omega_2)}{\sigma(t - \omega_2)\sqrt{\sigma(t-\gamma)\,\sigma(t-\beta)}} -\right.$$

$$\left. - 2\,\frac{[\sigma'(\Delta - t)\,\sigma(-t + \delta + \omega_2) - \sigma(\Delta - t)\,\sigma' \times}{\times(-t + \delta + \omega_2)]\,\sigma'(-t + \delta + \omega_2)}{\sigma(-t + \delta + \omega_2)\,\sigma(t - \omega_2)\sqrt{\sigma(t-\beta)\,\sigma(t-\gamma)}}\right\};$$

$$\Delta = \omega_1 - \delta + \frac{\gamma + \beta}{2}.$$

Let us extract expression for function z (u):

$$z(u) = \frac{1}{v_\infty} \int_0^u e^{-F(u)} \frac{dW}{du}\, du. \tag{8}$$

For the uniqueness of function z (u) let us require satisfaction of periodicity condition $z(u + 2\omega_1) = z(u)$, which can be presented in the form

$$\int_0^{2\omega_1} e^{-F(u)} \frac{dW}{du}\, du = 0. \tag{9}$$

Into the solution of problem entered the parameters α, β, γ, δ, ω_1/ω_2, A, τ, μ, $\frac{v_0}{v_\infty}$, H, l_1, l_2, for determining which we utilize equations (2), (5), (7), (8) and two equations, which correspond to the lengths of the plates:

$$l_1 \sin \mu = \frac{1}{v_\infty} \operatorname{Im} \int_0^\beta e^{-F(u)} \frac{dW}{du} du;$$

$$l_2 \sin (\mu + \tau) = \frac{1}{v_\infty} \operatorname{Im} \int_\gamma^{2\omega_1} e^{-F(u)} \frac{dW}{du} du.$$

Thus, we obtain four-parameter family of solutions. Let us assign, for example,

$$\frac{v_0}{v_\infty}, \mu, H, \frac{e_1}{H_1}.$$

The complex pressure of flow on the wing

$$R = X - iY = -\oint p n ds,$$

where n is an external standard to streamline. By utilizing Bernoulli's integral and by transfer/converting into plane alternating/variable u, we will obtain

$$\overline{R} = -\frac{i\varrho}{2}\int_0^{2\omega_1} (v_0^2 - v^2)\frac{d\overline{z}}{du}du.$$

BIBLIOGRAPHY

1. Кузнецов А. В.— ПМТФ, 1963. 6.
2. Кузнецов А. В.— Изв. вузов, 1961, 4.
3. Седов Л. И. Плоские задачи гидродинамики и аэродинамики, ГИТТЛ, М., 1960.
4 Уиттекер Э. Т., Ватсон Дж. Н. Курс современного анализа, II, М.— Л., 1963.
5. Harlay D. E.— В кн.: Boundary layer and flow control, II, Edited by Lachmann, 1961.

MOTION OF LOW-ASPECT-RATIO WING NEAR THE INTERFACE OF THE LIQUIDS OF DIFFERENT DENSITIES.

S. I. Putilin.

(Kiev).

The task of the motion of low-aspect-ratio wing under free surface of liquid is investigated in A. N. Panchenkova's work [7]. By similar method in work [8] is obtained the integral equation of low-aspect-ratio wing, which moves above the interface of the liquids of different densities. In these works found the load distribution chordwise of wing. Is given below the solution of problem, which makes it possible to determine load distribution chordwise of wing for the mode/conditions, which satisfy condition $\lambda Fr^2 \longrightarrow 0$, where the Froude number is designed on the wingspan.

1. The velocity potential of the lifting surface, which moves above the interface of liquids, must satisfy the following boundary conditions of section (index 1 is related to upper, 2 - to lower

liquid):

$$\varrho_1(\Phi_{1xx}-\mu\Phi_{1x}+\nu\Phi_{1z})-\varrho_2(\Phi_{2xx}-\mu\Phi_{2x}+\nu\Phi_{2z})=0;$$
$$\Phi_{1z}=\Phi_{2z},$$

where $\nu = g/v^2$; v is a rate of wing. In the turned flow is directed to the side negative x.

Page 62.

By method of the potential of accelerations with the use of representation [5]

$$\frac{1}{\sqrt{(x-\xi)^2+(y-\eta)^2+(z-\zeta)^2}}=\frac{1}{2\pi}\int_{-\infty}^{\infty}\int_{-\infty}^{\infty}e^{-(z-\zeta)\sqrt{\lambda^2+k^2}+io}\,d\lambda dk,$$

where $\sigma = (x-\xi)\lambda + (y-\eta)k$, obtained following expression for Φ_1:

$$\Phi_1 = -\frac{1}{4\pi}\int_S\int \Gamma(\xi,\eta)\left\{\int_{\infty}^{x}\frac{\partial}{\partial\zeta}\left[\frac{1}{r}+\frac{1}{\pi}\int_{-\infty}^{\infty}\int_{-\infty}^{\infty}\frac{N(\lambda,k)}{Q(\lambda,k)}e^{i\lambda\tau}d\lambda dk\right]d\tau\right\}ds, \tag{1}$$

where

$$N = \frac{a}{2\sqrt{\lambda^2+k^2}}[\nu\sqrt{\lambda^2+k^2}-\lambda^2]e^{-\sqrt{\lambda^2+k^2}(z+\zeta)+ik(y-\eta)}; \tag{2}$$

$$Q = a\nu\sqrt{\lambda^2+k^2}-\lambda^2+i\mu\lambda; \tag{3}$$

$$a = \frac{\varrho_2-\varrho_1}{\varrho_2+\varrho_1}.$$

The roots of equation Q = 0 lie/rest at lower half-plane, and during integration in their final result necessary to go around on top. By transferring the duct of the integration to lower half-plane, we will obtain the asymptotic representation of velocity potential at

the large negative values of $x - \xi$:

$$\Phi_{-\infty} = -\frac{1}{4\pi}\int_S\int \Gamma(\xi, \eta)\left\{\int_{-\infty}^{\infty}\frac{\partial}{\partial\xi}\left(\frac{1}{r}\right)d\tau + 2\int_0^{\infty} e^{-k(z+\zeta)}\cos k(y-\eta)dk - \right.$$

$$\left. - \frac{2(1-a)}{\bar{\nu}}\int_{-\infty}^{\infty}\frac{\lambda_0^2}{\sqrt{\bar{\nu}^2+4k^2}}\, e^{-(z+\zeta)+ik(y-\eta)}\cos\lambda_0(x-\xi)\,dk\right\} ds,$$

where

$$\lambda_0^2 = \frac{\bar{\nu}^2}{z} + \frac{\bar{\nu}^2}{2}\sqrt{\bar{\nu}^2+4k^2};$$

$$\bar{\nu} = a\nu.$$

By introducing the dimensionless quantities

$$\bar{\omega} = \bar{\nu} b; \qquad h = \frac{\zeta}{2b}; \qquad \gamma = \frac{\Gamma}{v_0}; \qquad \varphi = \frac{\Phi}{v_0 b} \tag{4}$$

and by relating x and ξ to half chord, but y, η , z, ζ - to semirange, we will obtain after simple conversions the integral equation

$$\varphi_z = -\frac{1}{2\pi\bar{\lambda}} \int_{-1}^{+1} \int_{x}^{1} \gamma_1(\xi)\, \gamma_2(\eta) \left\{ \frac{1}{y-\eta} - \int_0^\infty e^{-4kh} \sin k(y-\eta) dk + \right.$$

$$+ \bar{\omega}(1-a) \int_0^\infty \frac{t+1}{t} e^{-4h\bar{\omega}(t+1)} \sin\left[\bar{\omega}\sqrt{t(t+1)}\,(y-\eta)\right] \times$$

$$\left. \times \sin\left[\frac{\bar{\omega}}{\bar{\lambda}}(x-\xi)\sqrt{t+1}\right] dt \right\} d\xi d\eta, \tag{5}$$

where accepted

$$\gamma(\xi, \eta) = \gamma_1(\xi)\,\gamma_2(\eta) \quad \text{и} \quad \int_{-1}^{+1} \gamma_1(\xi)\,d\xi = 2. \tag{6}$$

Page 63.

For the flat/plane plate of low elongation in infinite liquid solution it is

$$\gamma_1(\xi) = \delta(\xi - 1).$$

It is possible to expect that and near the interface of the liquids cf different densities basic part of the load will concentrated on leading edge, and accept

$$\int_x \gamma_1(\xi) \cos[\bar{\omega}(x - \xi)]\,d\xi = 2.$$

After this simplification equation (5) assumes the form of the equation of finite-span wing with the optimum load distribution,

solved A. N. Panchenkov and P. I. Zinchuk [6].

Applying the obtained in this work results, we have

$$\gamma_2(y) = \lambda\sqrt{1-y^2}(A_1 + A_2y^2 + A_3y^4 + \ldots),$$

where A_i they depend on insertion they are expressed as special functions $G_{sp}(\frac{\bar{\omega}}{\tau})$. The expressions, which determine forces, are given in work [8].

Page 64.

2. In monograph [6] obtained common/general/total expression of the velocity potential of the lifting surface, which moves above the interface of the liquids of different densities. This expression can be rewritten in the following form:

$$\varphi = -\frac{1}{4\pi\lambda}\int_{-1}^{+1}\int_{-1}^{+1}\gamma(\xi,\eta)\left\{\frac{z-\zeta}{(y-\eta)^2+(z-\zeta)^2}\times\right.$$

$$\times\left[\frac{(x-\xi)\lambda^{-1}}{\sqrt{(x-\xi)^2\lambda^{-2}+(y-\eta)^2+(z-\zeta)^2}}-1\right]-\frac{z+\zeta}{(y-\eta)^2+(z+\zeta)^2}\times$$

$$\times\left[\frac{(x-\xi)\lambda^{-1}}{\sqrt{(x-\xi)^2\lambda^{-2}+(y-\eta)^2+(z+\zeta)^2}}-1\right]-\frac{1-a}{2\pi i}\left[\int_{-\frac{\pi}{2}}^{\frac{\pi}{2}}\int_{L_1}\frac{k\cos\theta}{k\cos^2\theta-\bar{\omega}}\times\right.$$

$$\times e^{-k(z+\zeta-i\sigma)}dkd\theta-\int_{-\frac{\pi}{2}}^{\frac{\pi}{2}}\int_{L_1}\frac{k\cos\theta}{k\cos^2\theta-\bar{\omega}}e^{-k(z+\zeta+i\sigma)}dkd\theta\Bigg]-$$

$$-2(1-a)\bar{\omega}\int_{-\frac{\pi}{2}}^{\frac{\pi}{2}}e^{-\frac{\bar{\omega}(z+\zeta)}{\cos^2\theta}}\cos\left[\frac{\bar{\omega}}{\cos\theta}\frac{x-\xi}{\lambda}+\frac{\bar{\omega}\sin\theta}{\cos^2\theta}(y-\eta)\right]\left.\frac{d\theta}{\cos^3\theta}\right\}d\eta d\xi, \tag{7}$$

where

$$\sigma = \frac{x - \xi}{\lambda} \cos\theta + (y - \eta) \sin\theta. \qquad (8)$$

Are here introduced dimensionless quantities by formulas (4). Duct L_2 goes around singular point $k = \frac{\bar{\omega}}{\cos^2\theta}$ from below, duct L_1 - on top.

I investigate the behavior of derivative φ_x with $\lambda \to 0$, $x < \xi$. The first two members are studied in work [2]. Evaluations for double integrals can be obtained by the method of consecutive integration in parts [9] which leads to this series:

$$-\int_{-\frac{\pi}{2}}^{\frac{\pi}{2}} \int_{L_j} f(k)\, e^{-k(z+\zeta \pm i\sigma)}\, dk d\theta \approx -\sum_{n=0}^{\infty} \int_{-\frac{\pi}{2}}^{\frac{\pi}{2}} f^{(n)}(0)\, (z + \zeta \pm i\sigma)^{-1-n} d\theta.$$

Here positive sign corresponds to duct L_1, and sign "minus" - to duct L_2:

$$f(k) = \frac{k^2 \cos\theta}{k\cos^2\theta - \omega}.$$

The first nonzero member is obtained with n = 2. He is of the order λ^3:

$$A_1 = \frac{2}{\omega} \int_{-\frac{\pi}{2}}^{\frac{\pi}{2}} \frac{\cos\theta d\theta}{\left\{z + \zeta \pm i\left[\frac{x-\xi}{\lambda}\cos\theta + (y-\eta)\sin\theta\right]\right\}^3}.$$

The evaluation of the last/latter term can be obtained from the method of steady state [3], [9]. For the integral

$$I = \int_{-\frac{\pi}{2}}^{\frac{\pi}{2}} e^{\frac{\bar{\omega}(z+\zeta)}{\cos^2\theta}} \cos\left[\frac{\bar{\omega}(x-\xi)}{\lambda} H(\theta)\right] \frac{d\theta}{\cos^5\theta}$$

the determining points are the points, where $H'(\theta) = 0$. In our case

$$H(\theta) = \frac{1}{\cos\theta} + \frac{\lambda(y-\eta)}{x-\xi} \frac{\sin\theta}{\cos^2\theta}$$

and the stationary points are determined by the formula

$$\sin^2\theta = \frac{1-2d^2 \pm \sqrt{1-8d^2}}{2(1-d^2)},$$

where

$$d = \lambda \frac{y-\eta}{x-\xi}.$$

From four values of sine θ it is necessary to select those whose sign is opposite to sign d. Considering λ low and reject/throwing the terms whose order λ^3 is above, we will obtain

$$\sin^2\theta_1 = 1-4d^2; \qquad \sin\theta_2 = -d.$$

The term of asymptotic expansion, which corresponds to root θ_1, will contain the factor exp $\left[-\frac{\bar{\omega}(z+\bar{\zeta})}{4d^2}\right]$ and it can be lowered. To root θ_2 corresponds term

$$I \approx e^{-\bar{\omega}(z+\zeta)} \sqrt{\frac{2\pi\lambda}{\bar{\omega}|x-\xi|}} \cos\left[\frac{\bar{\omega}|x-\xi|}{\lambda} + \frac{\pi}{4}\right]. \qquad (9)$$

Reject/throwing into φ_2 the terms, the order of smallness of which is higher than λ, we will obtain the equation

$$\lambda a(x, y) = -\frac{1}{2\pi}\int_{-1}^{+1}\int_{x}^{1} \gamma_\eta(\xi, \eta)\left[\frac{1}{y-\eta} - \frac{y-\eta}{(y-\eta)^2+16h^2}\right]d\xi d\eta +$$

$$+ \frac{(1-a)\bar{\omega}^2}{2\pi}\int_{-1}^{+1}\int_{x}^{1} \gamma(\xi, \eta)\, e^{-4h}\sqrt{\frac{2\pi\lambda}{\bar{\omega}|x-\xi|}}\cos\left[\frac{\bar{\omega}|x-\xi|}{\lambda} + \frac{\pi}{4}\right]d\xi d\eta. \qquad (10)$$

Integration for ξ is spread to cut $x < \xi < 1$, since with the taken degree of accuracy $\varphi_z = 0$ with $x > \xi$.

We will be restricted to the case, when angle of attack is not changed on spread/scope; function $\gamma(\xi, \eta)$ let us search for in the form of the product

$$\gamma(\xi, \eta) = \gamma_1(\xi)\,\gamma_2(\eta).$$

Of three terms of equation (10) only one depends on y, which reduces to the equation

$$\int_{-1}^{+1} \gamma_2^1(\eta)\left[\frac{1}{y-\eta}-\frac{y-\eta}{(y-\eta^2)+16h^2}\right]d\eta = \text{const}. \qquad (11)$$

Expression (11) takes the form of the equation of finite-span wing with the optimum load distribution, which moves above the screen. The solution to this equation obtained in work [6] in the form of the series

$$\gamma_2(y) = \sqrt{1-y^2}(A_1 + A_2y^2 + A_3y^4 + \ldots),$$

where of the function A_i is expressed as the parameter $\tau = \sqrt{4h^2+1} - 2h$. Hence, after placing constant in equation (11) equal to 1, we will obtain

$$\int_{-1}^{+1} \gamma_2(\eta)\,d\eta = \pi\left(1+\frac{1}{2}\tau^2+\frac{1}{4}\tau^4+\frac{7}{16}\tau^6+\ldots\right)=\pi\psi(h).$$

Taking into account the aforesaid equation (10) is copied in the form

$$\lambda a(x) = \int_x^1 \gamma_1(\xi)\, d\xi + \frac{1}{2}(1-a)\,\bar{\omega}^2\psi(h)e^{-4h\bar{\omega}} \int_x^1 \gamma_1(\xi) \times$$
$$\times \sqrt{\frac{2\pi\lambda}{\bar{\omega}(\xi - x)}} \cos\left[\frac{\bar{\omega}(\xi - x)}{\lambda} + \frac{\pi}{4}\right] d\xi.$$

The replacement of variables $\xi = \lambda\ (1 - r)$, $x = \lambda\ (1 - t)$ reduces this equation to the form

$$\int_0^t \gamma_1(\tau)\, d\tau - \mu \int_0^t \gamma_1(\tau)\, K(t-\tau)\, d\tau = \alpha(t), \qquad (12)$$

where

$$\frac{\gamma^*(p)}{p} - \frac{\mu}{p} K^*(p)\, \gamma^*(p) = \alpha^*(p). \qquad (13)$$

This equation can be solved by the method of the conversion of laplasa - Carson [4].

Page 67.

By designating the images of functions by asterisks, we will obtain

AD-A045 931 FOREIGN TECHNOLOGY DIV WRIGHT-PATTERSON AFB OHIO F/G 20/4
HYDRODYNAMICS OF LIFTING SURFACES (SELECTED ARTICLES).(U)
MAY 77

UNCLASSIFIED FTD-ID(RS)T-0784-77 NL

2 OF 2
ADA
045931

END
DATE
FILMED
11-77
DDC

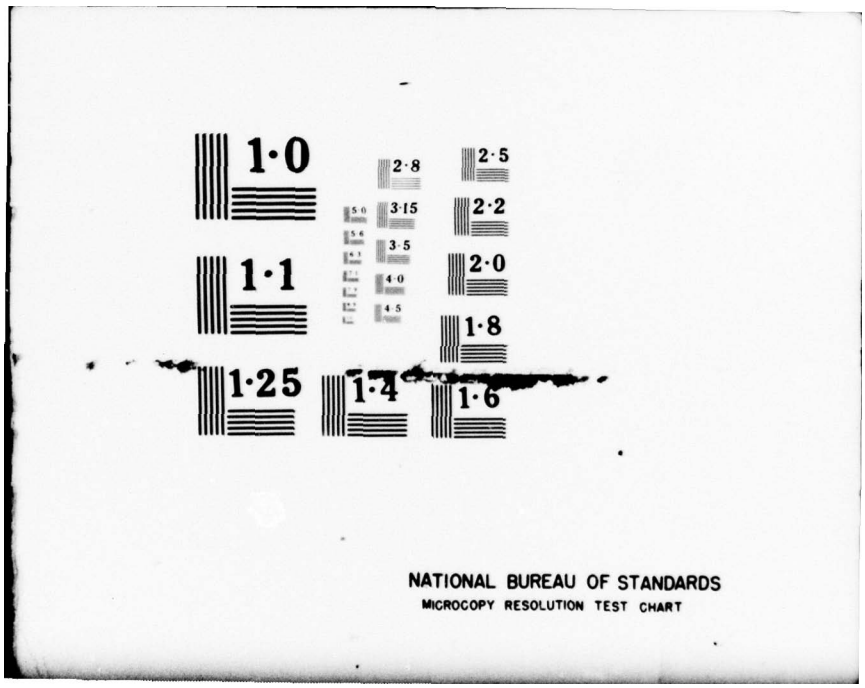
1·0
1·1
1·25
1·4
1·6
1·8
2·0
2·2
2·5
2·8
3·15
3·5
4·0
4·5
5·0
5·6
NATIONAL BUREAU OF STANDARDS
MICROCOPY RESOLUTION TEST CHART

$$\gamma^*(p) = \frac{p\alpha^*(p)}{1 - \mu K^*(p)},$$

whence

$$p\alpha^*(p) \div \alpha'(t) + \alpha(0)\,\delta(t).$$

Introducing function $\Phi(t) = \int_0^t \gamma(\tau)\,d\tau$ and taking into consideration that

$$\mu = \frac{1}{2}(1 - a)\,\bar{\omega}^2\psi(h)\,e^{-4h\bar{\omega}};$$

$$K(t) = -\sqrt{\frac{2\pi}{\bar{\omega}t}}\cos\left(\bar{\omega}t + \frac{\pi}{4}\right),$$

we will obtain

$$\Phi^*(t) = a(0)\,v(t) + \int_0^t a'(\tau)\,v(t-\tau)\,d\tau, \qquad (14)$$

where function v (t) it is determined from its image:

$$v^*(p) = \frac{1}{1-\mu K^*(p)}. \qquad (15)$$

The total wing characteristics can be expressed directly through $\Phi(t)$, therefore task will be solved, if we determine resolvent v (t).

3. Analogously it is possible to study the case of the wing, which moves under the interface of two liquids. By utilizing results [4], we will obtain for a velocity potential the expression, similar to expression (7):

$$\varphi = -\frac{1}{4\pi\lambda}\int_{-1}^{+1}\int_{-1}^{1}\gamma(\xi,\eta)\left\{\frac{z-\zeta}{(y-\eta)^2+(z-\zeta)^2}\times\right.$$

$$\times\left[\frac{(x-\xi)\lambda^{-1}}{\sqrt{(x-\xi)^2\lambda^{-2}+(y-\eta)^2+(z-\zeta)^2}}-1\right]-\frac{z+\zeta}{(y-\eta)^2+(z+\zeta)^2}\times$$

$$\times\left[\frac{(x-\zeta)\lambda^{-1}}{\sqrt{(x-\xi)^2\lambda^{-2}+(y-\eta)^2+(z-\zeta)^2}}-1\right]-$$

$$-\frac{(1+a)}{2\pi i}\left[\int_{-\frac{\pi}{2}}^{\frac{\pi}{2}}\int_{L_1}\frac{k\cos\theta}{k\cos^2\theta-\bar{\omega}}e^{k(z+\zeta+i\sigma)}dkd\theta-\int_{-\frac{\pi}{2}}^{\frac{\pi}{2}}\int_{L_1}\frac{k\cos\theta}{k\cos^2\theta-\bar{\omega}}\times\right.$$

$$\left.\times e^{k(z-\zeta-i\sigma)}dkd\theta\right]-2(1+a)\bar{\omega}^2\int_{-\frac{\pi}{2}}^{\frac{\pi}{2}}e^{\frac{\bar{\omega}(z+\zeta)}{\cos^2\theta}}\cos\left[\frac{\bar{\omega}(x-\xi)}{\lambda\cos\theta}H(\theta)\right]\times$$

$$\left.\times\frac{d\theta}{\cos^2\theta}\right\}d\xi d\eta. \qquad (16)$$

The comparison of formulas (7) and (16) shows that the final equation for this case differs from equation (12) only in terms of value of value μ, which must be replaced with value

$$\mu_1 = -\frac{1}{2}(1+a)\bar{\omega}^2\psi(h)\,e^{-4/\bar{\omega}}.$$

4. Asymptotic expression (13) of nucleus K (t) with an accuracy down to the terms of order $\lambda^{3/2}$ can be replaced with the expression

$$K(t) = \pi J_1(t),$$

where J_1 is a Bessel function. Then for the image of resolvent we obtain

$$v^*(p) = \frac{1}{1-\mu\pi\dfrac{p(\sqrt{p^2+\bar{\omega}^2}-p)}{\bar{\omega}\sqrt{p^2+\bar{\omega}^2}}}.$$

Bringing this expression to the form

$$v^*(p) = \frac{P_2}{P_1} + \frac{p}{\sqrt{p^2+\bar{\omega}^2}} \cdot \frac{P_3}{P_1},$$

where

$$P_1 = 2\pi\mu p^3 - p^2\bar{\omega}(1 + \pi^2\mu^2) + 2\pi\mu\bar{\omega}^2 p - \bar{\omega}^3;$$

$$P_2 = \mu\pi p^3 - p^2\bar{\omega} + \pi\mu\bar{\omega}^2 p - \bar{\omega}^3;$$

$$P_3 = \pi\mu p\,(p^2 + \bar{\omega}^2),$$

we will obtain

$$v(t) = \sum_{n=1}^{3} \left\{ \frac{P_2(p_n)}{P_1'(p_n)} e^{p_n t} + \frac{P_3(p_n)}{P_1'(p_n)} \left[J_0(\bar{\omega}t) + p_n \int_0^t J_0(\bar{\omega}\tau) e^{p_n(t-\tau)} d\tau \right] \right\}.$$

where p_n are roots of equation $P_1(p) = 0$.

In the case of infinite liquid $\mu = 0$, $v(t) = 1$ we obtain

$$\Phi(t) = \alpha(t).$$

If function $\alpha(t)$ is continuous, then $\Phi(t)$ also continuous and limited with $t > 0$, in particular on trailing wing edge, which provides satisfaction of zhukovskiy - Chaplygin's condition [9]. It is easy to see that the equation of nonpassage will not be disturbed, if we on trailing wing edge place the eddy/vortex of the final intensity Γ. If we assume $\Gamma = -\Phi(\frac{2}{\lambda})\gamma_2(\eta)$, then we will obtain the case of noncirculating flow.

BIBLIOGRAPHY

1. Белоцерковский С. М. Тонкая несущая поверхность в дозвуковом потоке газа. «Наука», М., 1965.
2. Задачи и методы гидродинамики подводных крыльев и винтов. «Наукова думка», К., 1966.
3. Костюков А. А. Теория корабельных волн и волнового сопротивления. Судпромгиз, Л., 1959.
4. Лурье А. И. Операционное исчисление. Гостехиздат, М., 1950.
5. Морс Ф. М., Фешбах Г. Методы теоретической физики, т. 2. ИЛ, М., 1960.
6. Панченков А. Н. Гидродинамика подводного крыла. «Наукова думка», К., 1965.
7. Панченков А. Н.— В кн.: Исследования по прикладной гидромеханике. «Наукова думка», К., 1965.
8. Путилин С. И.— В кн.: Гидродинамика больших скоростей, 1. «Наукова думка», К., 1965.
9. Эрдейи А. Асимптотические разложения. Физматгиз, М., 1960.

INTERFERENCE OF AIRFOIL/~~PROFILES~~ IN A SUBSONIC UNSTEADY FLOW.

V. B. Kurzin.

(Novosibirsk).

Page 188.

The interference of airfoil/profiles in the compressed unsteady flow theoretically was investigated for an infinite grid/cascade. Specifically, for the study of the case of the subsonic of the unsteady flow of grid/cascade of the author was used the method of integral equations [2]. This method can be extended to the more general case of subsonic unsteady flow of liquid relative to system from the finite number of airfoil/profiles. As an example was examined the flow about the biplane and was carried out the calculation of the unsteady aerodynamic forces, acting on its airfoil/profiles. The obtained results can be used for the analysis of the forces, which act on airfoil/profile near the interface of two media.

Let us examine system from N of the fine/thin slightly

bent/curved airfoil/profiles, which are located at low angle of attack in the flat/plane subsonic flow of gas and which accomplish arbitrary low harmonic oscillations (Fig. 1). The flow of gas in this case is described by the system of the integral equations of the form

$$v_{yl}(x_l, y_l) = \frac{\omega}{qU^2} \sum_{n=1}^{N} \int_{a_n}^{b_n} L_n(x_0, y_n) \frac{iM}{4\beta k} \exp\left[-\frac{ik(x_j - x_0)}{M}\right] \times$$
$$\times \int_{-\infty}^{x_j - x_0} \exp\left(\frac{ik\xi}{M\beta^2}\right) \frac{\partial^2}{\partial y^2}\left[H_0^{(2)}\left(\frac{k\sqrt{\xi^2 + \beta^2(y_j - y_n)^2}}{\beta^2}\right)\right] d\xi dx_0, \quad (1)$$

where

$$k = \frac{\omega b}{a}; \quad M = \frac{U}{a}; \quad \beta^2 = 1 - M^2; \quad i = 1, 2, \ldots, N.$$

Page 189.

Here x_j, y_j are coordinates of the points of the j airfoil/profile in the coordinate system, connected with one of the airfoil/profiles (see Fig. 1); a_n, b_n respectively the coordinate of

the leading and trailing edges of the n airfoil/profile; b - half cord of one of airfoil/profiles; ρ, U - respectively the density and the speed of flow; a - the speed of sound in undisturbed flow; ω is an angular oscillation/vibration frequency; v_{yj} - the amplitude vertical of the velocity component of the motion of the points of the j airfoil/profile; $L_n(x_0, y_n)$ - the amplitude of the distributed lift on the n airfoil/profile; $H_0^{(2)}(r)$ is a function of Hankel of the second zero-order kind.

As an example let us examine the unsteady flow of biplane (Fig. 2). Let us assume that the airfoil/profiles of biplane oscillate with identical forms and amplitudes. Then the system of integral equations (1) degenerates into one:

$$v_y(x) = \frac{\omega b}{\varrho U^2} \int_{-1}^{1} L(x_0) K(x - x_0)\, dx_0, \qquad (2)$$

nucleus of which it takes the form

$$K(x-x_0)=\frac{iM}{4\beta k}e^{-i\frac{k}{M}(x-x_0)}\left\{\int_{-\infty}^{x-x_0}\exp\left(i\frac{k\xi}{M\beta^2}\right)\frac{\partial^2}{\partial y^2}\left[H_0^{(2)}\left(\frac{k\xi}{\beta^2}\right)\right]d\xi+\right.$$

$$\left.+e^{i\alpha}\int_{-\infty}^{x-x}\exp\left(i\frac{k\xi}{M\beta^2}\right)\frac{\partial^2}{\partial y^2}\left[H_0^{(2)}\left(\frac{k}{\beta^2}\sqrt{\xi^2+\beta^2(y-h)^2}\right)\right]d\xi\right\}, \quad (3)$$

where h = H/b; a is a phase displacement between the oscillations of airfoil/profiles. For the numerical solution of integral equation (2) it is necessary to separate the special feature/peculiarities of nucleus. They coincide with the special feature/peculiarities of the kernel of integral equation of Possio and take the form

$$K(x-x_0)=-\frac{\beta M}{k(x-x_0)}+\frac{i}{\beta}\ln(x-x_0)+k_1(x-x_0). \quad (4)$$

For simplification in the calculation the regular part of nucleus k_1 we approximate with the aid of the trigonometric series

$$k_1(x-x_0)=\sum_{l=1}^{10}b_l\sin l\pi(x-x_0)+\sum_{l=0}^{10}c_l\cos l\pi(x-x_0). \qquad (5)$$

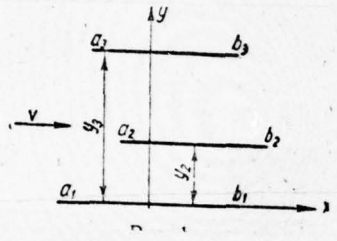

Fig. 1.

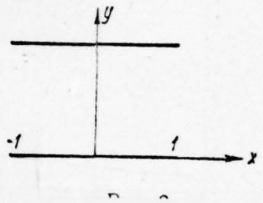

Fig. 2.

Page 190.

The solution to integral equation, as in the case of grid/cascade [2], we search for by collocation. For this purpose the unknown function let us present in the form of the series

$$L(x)=a_0\sqrt{\frac{1-x}{1+x}}+\sum_{n=1}^{N}a_n\sin\frac{n\pi}{2}(x+1). \qquad (6)$$

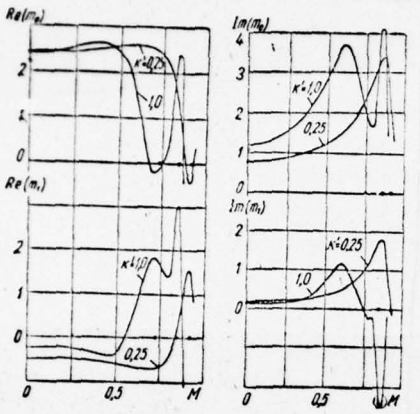

Fig. 3

By substituting expressions (4) - (6) in equation (2) and by fulfilling equality with N + 1 different values x, we will obtain N + 1 algebraic equation for determining the unknown constants a_η. In the calculation conducted integral equation was satisfied at nine points, evenly arrange/located chordwise of airfoil/profile.

For the illustration of compressibility effect on the aerodynamic interference of airfoil/profiles let us give some results of calculations. Aerodynamic forces and the torque/moments, which act on the airfoil/profiles of biplane, let us present in the form

$$P_y = \varrho U^2 b\,[l_0 + e^{i\alpha} l_1];$$
$$M = \varrho U^2 b^2\,[m_0 + e^{i\alpha} m_1]. \quad (7)$$

where l_j, m_j - influence coefficients for the j airfoil/profile (j = 0, 1) during the oscillations of the initial airfoil/profile (j = 0) according to the assigned law. They do not depend on phase displacement a and with the aid of expressions (7) can be determined from the solution to equation (2) for two different values of a.

On Fig. 3 for case of h = 2 are represented to the dependence of the influence coefficients of moment with respect to rotational axis for torsional oscillations about the middle of airfoil/profile on Mach number at the fixed values of Strouhal number $k^1 = k/M = 0.25$; 1.0. On the axis of ordinates for a comparison points plotted/applied corresponding values of influence coefficients, obtained in work [2] for the case of the incompressible fluid. From curve/graphs it is evident that at the determined values of Mach numbers the aerodynamic coefficients have sharply pronounced extrema. It turned out that these values of Mach numbers, determined from equation $2k/\beta^2 = mv$ (m = 1, 2, 3, ...), correspond to some special feature/peculiarities of the solution of problem.

Page 191.

These special feature/peculiarities make determined physical sense. At the indicated values of Mach number the oscillatory period is multiple the transit time of the plane wave of slight disturbance from the leading edge of airfoil/profile along flow to the rear and vice versa, i.e., occurs aerodynamic resonance. On the axis of abscissas cross plotted/applied the resonance values of Mach number for $k' = 0.25$, by points - for $k' = 1.0$.

On Fig. 4 for case of $h = 1$ are represented to the dependence of the influence coefficients of forces for the torsional oscillations of airfoil/profiles on Strouhal number k' at the fixed values of Mach number (curve with $M = 0$ is taken from work [2]).

On Fig. 5 is represented the dependence of the influence coefficient of force for the case of torsional oscillations on the distance between airfoil/profiles h at the fixed values of Mach number and of Strouhal number $k' = 1$.

The analysis of the obtained results shows that to the

interference of airfoil/profiles in unsteady flow the compressibility of liquid exerts a substantial influence at high subsonic speeds or high oscillation/vibration frequencies. If the wavelength of disturbance/perturbation ($l=\frac{2\pi}{\omega}a$) is commensurable with the characteristic geometric sizes of biplane, then essential effect on aerodynamic forces exerts the acoustic interaction of the oscillating airfoil/profiles.

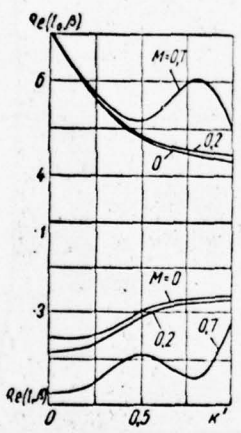

Fig. 4.

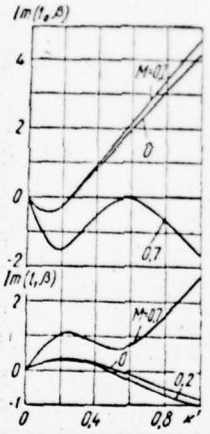

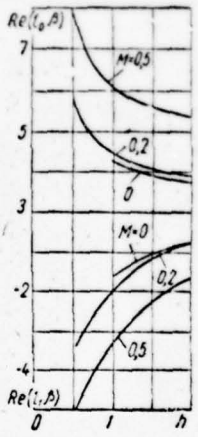

Fig. 5.

BIBLIOGRAPHY

1. Горелов Д. Н.— Изв. АН СССР. ОТН. Механика и машиностроение, 1964, 5.
2. Курзин В. Б.— ПМТФ, 1964, 2.

Page 223.

Calculation of landings of aerodynamic air-cushion vehicle, which starts from water.

V. I. Rudomanov.

(Kiev).

During the study of the motion of the apparatuses, which use a proximity effect of liquid or solid screen (aerodynamic air-cushion vehicles), special interest are of transient condition, which include the trajectory phases from start to the set of certain minimum speed, upon achieving which the aerodynamic air-cushion vehicle has sufficient aerodynamic controllability, and sections, on which the speed of aerodynamic air-cushion vehicle decreases from the minimum to zero.

In the general case transient condition being unsteady are characterized by effect on the aerodynamic air-cushion vehicle of the unsteady aerodynamic forces and thrust of power plant. To the aerodynamic air-cushion vehicle, which starts from water and which

has hydrofoils, supplementarily affect the unsteady flow forces, whereupon with the output/yield of aerodynamic air-cushion vehicle from water with an increase in the velocity the effectiveness of aerodynamic forces grows, and hydrodynamic - it falls.

Effect on the aerodynamic air-cushion vehicle of the unsteady forces produces change in the time of the parameters of motion, which determine the speed of aerodynamic air-cushion vehicle and its position in space.

If we approximately consider the longitudinal unsteady motion of aerodynamic air-cushion vehicle in transient condition as being quasi-steady, i.e., at the fixed/recorded moments of time to consider motion establish/installed, then the longitudinal unguided motion of aerodynamic air-cushion vehicle will be determined by these parameters: height/altitude H, by pitch angle ϑ and by speed v.

Let us examine the unguided axial motion of the aerodynamic air-cushion vehicle, which has forepart/nose and feed air and hydrofoils.

Page 224.

For simplification let us accept the following assumptions:

1) the resistance of aerodynamic air-cushion vehicle is balanced by the thrust/rod of power plant, and in this case is not created torque/moment, i.e., is examined the quasi-steady motion;

2) at the moments of time in question the flight path angle to the horizon θ = const = 0;

3) is absent mutual wing influence;

4) we disregard the center-of-pressure travel of hydrofoils chordwise during a change in altitude above the screen and of angle of attack, since this displacement considerably less than the arm of flow forces relative to the center of gravity of aerodynamic air-cushion vehicle.

Taking into account the adopted assumptions of the equation of the equilibrium of the aerodynamic air-cushion vehicle it is possible to write in this form:

$$\Sigma Y_i = G; \quad (1)$$

$$\Sigma Y_i L_i = 0. \quad (2)$$

For the apparatus, which has air and hydrofoils, it is possible to conditionally consider one wing system of basic (carrier), and another - auxiliary (unloading). Since for the aerodynamic air-cushion vehicle, which starts from water, basic is the state of motion on air wings, it is possible to conditionally count that the basic carrying wing system is the system of air wings despite the fact that in the beginning of transient condition with start basic load receive the hydrofoils.

The determination of landings of aerodynamic air-cushion vehicle, i.e., the calculation of dependences H (t) and ϑ (t), by the assigned values of velocity conducts by the method successive approximation as follows.

From equations (1) and (2) we obtain expressions for the coefficients hoisting forces of the air wings, required for the realization of the quasi-steady straight flight at given speed. In

the first approximation, is not considered discharging aerodynamic air-cushion vehicle by hydrofoils and the center-of-pressure travel of aerodynamic forces. After assigning several values of relative distance from the screen of air feed $(\bar{h}_{в.к})$ and air forepart/nose $(\bar{h}_{в.н})$wings, we determine dependence $\bar{h}_{в.н}$ (ϑ) $_1$. Utilizing a geometric relationship/ratio between $\bar{h}_{в.н}$ and $h_{в.к}$, we convert $\bar{h}_{в.н}$ (ϑ) and $\bar{h}_{в.к}$ (ϑ) $_2$. The unknown values $\bar{h}_{в.к}$ and ϑ, which correspond to equilibrium of forces, which act on aerodynamic air-cushion vehicle, are located from the solutions to the equations, which express dependence $\bar{h}_{в.к}$ (ϑ) $_1$ and $\bar{h}_{в.к}$ (ϑ) $_2$. From those which were found $\bar{h}_{в.к}$ and ϑ, utilizing obvious geometric relationship/ratios, we determine the bias of the cent of the pressure aerodynamic forces and a decrease of the weight of aerodynamic air-cushion vehicle as a result of discharging by hydrofoils.

Page 225.

We produce the calculation according to the second approach/approximation taking into account a decrease in weight and center-of-pressure travel. The values $\bar{h}_{в.к_i}$ and ϑ_i, obtained in the i approach/approximation, we compare with the values $\bar{h}_{в.к_{i-1}}$ and ϑ_{i-1}, obtained in (i-1) m approach/approximation, and we conclude the calculation upon reaching of the required accuracy/precision, i.e., with $|\bar{h}_{в.к_i} - \bar{h}_{в.к_{i-1}}| < \varepsilon_1; \quad |\vartheta_i - \vartheta_{i-1}| < \varepsilon_2.$

Since the presence of the system of air and hydrofoils predetermines the large volume of calculating works, it is expedient the calculation of landings to perform with the application/use of computer technology.

On Fig. 1 is given the block diagram of solution by ETsVM [- digital computer] of the task of the calculation of landings of the aerodynamic air-cushion vehicle, which starts from water. This block diagram can be used also by manual calculations and the calculation of landings with the aid of simulators. For the calculation of landings is utilized the following formula:

$$C_{y\text{потр}_{в.к}} = \frac{2G}{\varrho_1 S_{в.к} v^2} \cdot \frac{L_{в.н} - x_{в.н}}{L_{в.н} + L_{в.к} - x_{в.н} + x_{в.к}} -$$

$$- \frac{\varrho_2 S_{н.н}}{\varrho_1 S_{в.к}} \cdot \frac{L_{в.н} - L_{п.н} - x_{в.н}}{L_{в.н} + L_{в.к} - x_{в.н} + x_{в.к}} C_{y_{п.н}} -$$

$$- \frac{\varrho_2 S_{п.к}}{\varrho_1 S_{в.к}} \cdot \frac{L_{п.к} + L_{в.н} - x_{в.н}}{L_{в.н} + L_{в.к} - x_{в.н} + x_{в.к}} C_{y_{п.к}};$$

$$C_{y\text{потр}_{в.н}} = \frac{2G}{\sigma_1 S_{в.н} v^2} \cdot \frac{L_{в.к} + x_{в.к}}{L_{в.н} + L_{в.к} - x_{в.н} + x_{в.к}} -$$

$$- \frac{\varrho_2 S_{п.к}}{\varrho_1 S_{в.н}} \cdot \frac{L_{п.к} - L_{п.к} + x_{в.к}}{L_{в.н} + L_{в.к} - x_{в.н} + x_{в.к}} C_{y_{п.к}} -$$

$$- \frac{\varrho_2 S_{п.н}}{\varrho_1 S_{в.н}} \cdot \frac{L_{п.н} + L_{в.к} + x_{в.к}}{L_{в.н} + L_{в.к} - x_{в.н} + x_{в.к}} C_{y_{п.н}};$$

$$C_y^a = \frac{a_\infty \psi}{c_2(\lambda)\left[1 + \frac{a_\infty \psi (1 + c_1(\lambda))}{\pi \lambda c_2(\lambda)} \xi\right]};$$

$$\psi_п = 1 - \tau^2 + \tau^4 - \frac{3}{4}\tau^6 + \frac{5}{8}\tau^8 - \frac{3}{8}\tau^{10};$$

$$\psi_в = \psi_0 [1 - \alpha \psi_0 \tau (1 + 0,5\tau^2)];$$

$$\psi_0 = \frac{1}{1 - \tau^2 + \frac{1}{4}\tau^4 - \frac{1}{4}\tau^6};$$

$$\tau = \sqrt{(2\bar{h})^2 + 1} - 2\bar{h};$$

$$\xi = 1 \pm (0,5\tau_\lambda^2 + 0,25\tau_\lambda^4 + 0,0625\tau_\lambda^6 + 0,0469\tau_\lambda^8 + + 0,0257\tau_\lambda^{10} + 0,0188\tau_\lambda^{12}).$$

where x is the expressed into the portions of the mean aerodynamic chord center-of-pressure travel of wing; a_∞ = const $\approx$ 5.45.

Page 226.

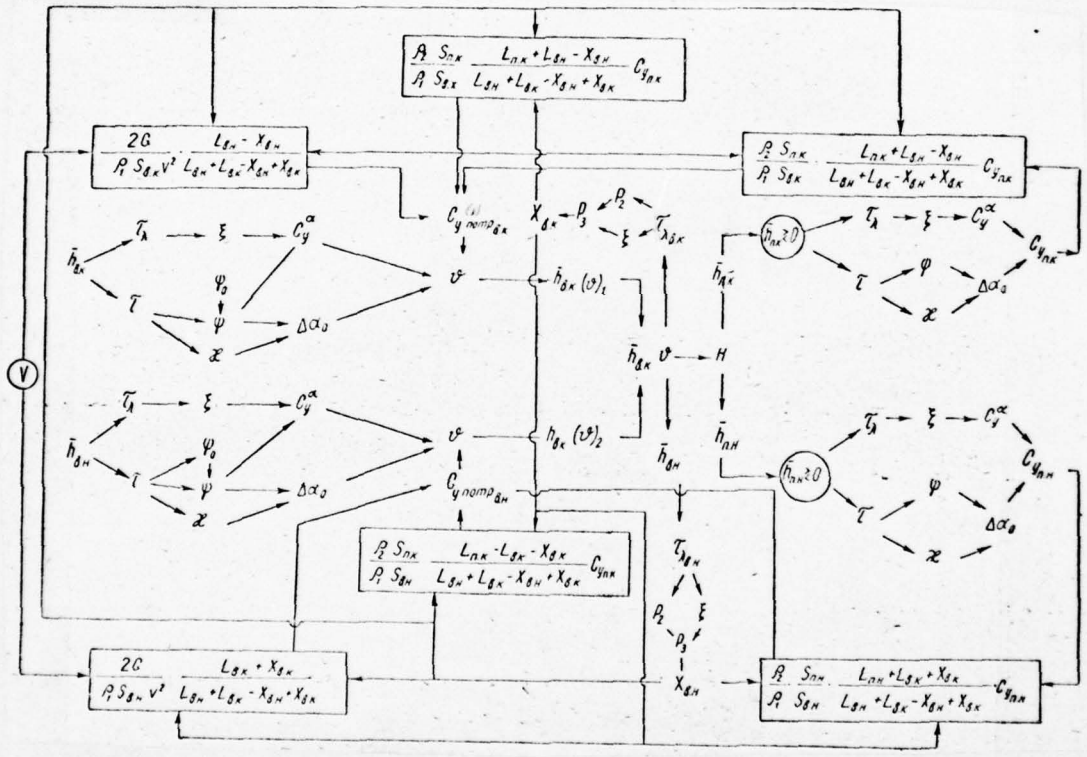

Fig. 1.

Page 227.

In the last/latter expression positive sign before the bracket is related to hydrofoil, "minus" - to air;

$$\tau_\lambda = \sqrt{\left(\frac{2\bar{h}}{\lambda}\right)^2 + 1} - \frac{2\bar{h}}{\lambda}.$$

Functions c_1 (λ) and c_2 (λ) take the following values (λ - wing aspect ratio):

λ	$c_1(\lambda)$	$c_2(\lambda)$
0	1,0000	0,0000
0,25	0,9371	0,3538
0,50	0,8781	0,5945
1,00	0,7710	0,7710
1,5	0,6740	0,8411
2,0	0,5945	0,8798
2,5	0,5220	0,9048
4,0	0,3534	0,9380
7,5	0,1422	0,9666
10	0,0743	0,9743
15	0,0202	0,9831
∞	0,0000	1,0000

$$C_y = C_y^{\alpha}(\alpha - \Delta\alpha_0 + \vartheta);$$

$$\Delta\alpha_0 = -\frac{\varkappa}{\psi}\alpha_0 + \frac{\bar{c}}{2}\frac{\tau^3}{\psi};$$

$$\varkappa = \frac{1}{2}\tau^2 - \tau^4 + \frac{13}{16}\tau^6 - \frac{5}{8}\tau^8 + \frac{5}{16}\tau^{10};$$

$$\vartheta = \frac{C_{y_{\text{потр}}}}{C_y^{\alpha}} + \Delta\alpha_0 - \alpha;$$

$$x = \frac{\frac{\lambda}{P_3}\operatorname{th}\left(\frac{2P_3}{\lambda}\right) - \frac{2}{\operatorname{ch}(2P_3/\lambda)}}{2\left[1 - \operatorname{ch}\left(\frac{2P_3}{\lambda}\right)\right]};$$

$$P_3 = \sqrt{8\frac{\bar{\xi}}{P_2}};$$

$$P_2 = 1 - \frac{1}{2}\tau_\lambda - \frac{7}{24}\tau_\lambda^3 - \frac{3}{32}\tau_\lambda^5 - \frac{1}{64}\tau_\lambda^7;$$

$$\operatorname{th}\left(\frac{2P_3}{\lambda}\right) = \frac{e^{\frac{2P_3}{\lambda}} - e^{-\frac{2P_3}{\lambda}}}{e^{\frac{2P_3}{\lambda}} + e^{-\frac{2P_3}{\lambda}}};$$

$$\operatorname{ch}\left(\frac{2P_3}{\lambda}\right) = \frac{e^{\frac{2P_3}{\lambda}} + e^{-\frac{2P_3}{\lambda}}}{2};$$

$$\bar{h}_n = \frac{H - (\Delta h_{o.в} + b_{o.в}\sin\alpha)_n \mp (L_{o.в} \pm b_{o.в}\cos\alpha)_n \operatorname{tg}\vartheta}{b_n};$$

$$h_n = \frac{(\Delta h_{o.в} + b_{o.в}\sin\alpha)_n - H \pm (L_{o.в} \pm b_{o.в}\cos\alpha)_n \operatorname{tg}\vartheta}{b_n},$$

where α is an angle of attack of wing; α_0 - zero-lift angle; $\Delta\alpha_0$ are a change in the angle of the zero zero lift of solid airfoil/profile due to the influence of screen.

In two last/latter formulas the upper signs are related to feed wings, lower - to forepart/nose;

$$H = \bar{h}_{в.к} b_{в.к} + (\Delta h_{о.в} + b_{о.в} \sin\alpha)_{в.к} + (L_{о.в} + b_{о.в} \cos\alpha)_{в.к} \operatorname{tg} \upsilon;$$

$$\bar{h}_{в.н} = \frac{\bar{h}_{в.к} b_{в.к} + (\Delta h_{о.в} + b_{о.в} \sin\alpha)_{в.к} + (L_{о.в} + b_{о.в} \cos\alpha)_{в.к} \operatorname{tg} \upsilon}{b_{в.н}} -$$

$$- \frac{(\Delta h_{о.в} + b_{о.в} \sin\alpha)_{в.н} - (L_{о.в} - b_{о.в} \cos\alpha)_{в.н} \operatorname{tg} \upsilon}{b_{в.н}}.$$

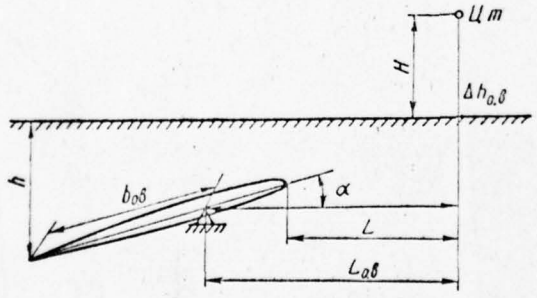

Fig 2.

Page 229.

The formulas, which express geometric relationship/ratios for the wings and the center of gravity (Fig. 2), considerably will be simplified, if wings are not turned during the motion of aerodynamic air-cushion vehicle.

BIBLIOGRAPHY

1 Басин А. М., Анфимов В. Н. Гидродинамика судна. «Речной транспорт», Л., 1961.
2. Егоров И. Т., Соколов В. Т. Гидродинамика быстроходных судов. «Судостроение», Л., 1965.
3. Панченков А. Н. Гидродинамика подводного крыла. «Наукова думка», К., 1965.
4. Панченков А. М.— В кн.: Проблеми гідромеханики судна. Вид-во АН УРСР, К., 1961.

EFFECT OF VORTEX FORMERS ON THE AERODYNAMIC WING CHARACTERISTICS AND BODY OF REVOLUTION

A. M. Mkhitaryan, S. A. Lukashuk, V. D. Trubenok, V. Ya. of Fridland.

(Kiev)

Page 254.

Vortex formers, which are deepenings (cavity) in the streamlined with fluid flow of rigid surface, attract attention already for 20 years.

Academician D. I. Blokhintsev [1] will give the analysis of the flow of ideal (by discrepancy) liquid in vortex former and its vicinities. It is shown, that the intensity of the eddy/vortex, which is conceived in cavity, builds up and eddy/vortex periodically will be carried by external flow downstream. The frequency of the generation of eddy/vortices can be sonic and ultrasonic. D. I. Blokhintsev investigated the phenomenon of resonance, when the natural frequency of liquid within cavity coincides with the frequency of the generation of eddy/vortices. On the basis of target/purposes and tasks of his investigations, D. I. Blokhintsev will call/name these cavities resonators. This name in essence will

be preserved also in the works of other authors, but their phenomenon of resonance interests already to a lesser degree. In the present work is utilized the term of "vortex former" more correctly, in our opinion, that reflects the essence of the phenomenon.

P. N. Kubanskiy [2, 3], utilizing vortex former for the intensification of heat exchange during the flow of the liquid about the beams of pipes it reveal/detected that under specific conditions hydrodynamic drag of the banks of tubes with smooth surface turns out to be greater than the resistance of tubes with vortex formers which was in experiments the cylindrical deepenings, drilled in the wall of tube.

Ob"yasneniye P. N. Kuban, datum to this strange at first glance phenomenon, lies in the fact that the eddy/vortices, generated by vortex formers form "cylinders", on which slips the boundary layer.

Page 255.

This lowers hydrodynamic drag of surface; however, energy additionally is expend/consumed on vortex formation. The total effect it can lead to a reduction/descent in hydrodynamic drag.

It is sufficiently in detail the physicist of the phenomena, connected with flow vortex formers is investigated V. K. Migaem [4. 5], who will study experimentally the flow pattern within vortex formers different size/dimensions, and also within plane diffuser with vortex formers and the flow about th cylindrical surface, placed in flat duct. It arrived at the conclusion that among the liquid within vortex former and the external flow occurs the intense turbulent mass exchange, in consequence of which near fairing is reconstructed the diagram/curve of rate, becoming more "complete". This it will direct V. K. Migaya to thought about use vortex formers for the stabilization of flows in diffusers with high downstream pressure gradients. For a cylindrical surface, in particular, they obtained the displacement of separation point from 24 to 35-38°.

In the laboratory of aerodynamics of the Kiev institute of the engineers of the civil aviation by the authors of this article were tested the conclusions V. K. Migaya and after their confirmation investigated the effect of vortex former on boundary-layer flow under conditions exterior problem. Experiments will confirm the possibility of the stabilization of the flow above the wing with high adverse pressure gradient. Vortex formers will allow to postpone the onset of the separation mode/conditicns of flow and thereby substantial to increase the critical angle of attack of airfoil/profile.

In the process of the blasting of finite-span wing the established fact of a reduction/descent in the effectiveness of vortex formers as a result of the three-dimensicnal character of flow. Almost completely it will be possible to restore/reduce effect by location in cavity of vortex formers partitien/baffle-separators.

For the practical target/purposes vortex formers most likely they can be used on the wings, equipped with flaps.

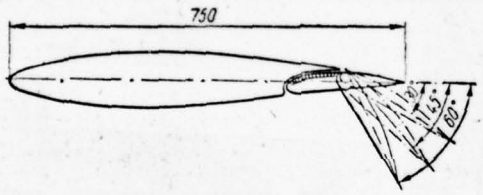

Fig. 1. Model of wing profile with flap for research on effect of vortex formers on the effectiveness of flap.

Page 256.

In this case in cruise setting the flap with vortex formers is clamped to wing (Fig. 1), vortex formers they do not affect wing characteristics. In takeoff and landing mode/conditions the flap is advanced back/ago, being simultaneously turned down around its rotational axis, and vortex formers begin to flow itself by the flow,

which penetrates through the slot between the wing and the flap.

For research on effect of vortex formers on the effectiveness of flap was made the two-dimensional experiment with the airfoil/profile with flap. Profile thickness $\bar{c}$ = 13o/o, chord b = 750 mm, the chord of flap $b_з$ = 228 mm. On the upper surface of the flap of six sections they will be interchangeable (Fig. 2), which makes it possible to establish/install vortex formers in different places chordwise. Are investigated vortex formers of two size/dimensions: I type is 2.5 X 5 mm and II type - 3.5 X 7 mm (first numeral is the width, the second - the depth of cavity vortex formers).

Experiment is carried out at the constant angle of attack of wing α = 10°. The models of wing and flap were drained in central cross section. Drain holes were provided for, also, in sections with vortex formers (on two holes in each section). They are located on the bottom of cavity, since the preceding/previous experiments showed that in this place the pressure is equalized up to a pressure of in external flow (diagram/curve of pressures it takes the form as smooth, monotonic curve without jumps and explosions).

Drain holes with the aid of flexible rubber hoses are connected with the tubes of the battery 70-point panel of piezometers. The rate in tube is measured by Pitot tube and is supported order 39-40 m/s.

Pressure and the temperature in working chamber constantly are record/fixed. The effectiveness of one set or the other of sections is determined by the comparison of values c_y during the identical units of the airfoil/profile of flap for flaps with smooth surface and system of vortex formers. The values c_y are determined by the measurement of the area of the diagram/curves of normal pressure on the wing surface and flap.

First of all was blown the model of wing - flap system in that form, in which they there exist without vortex formers.

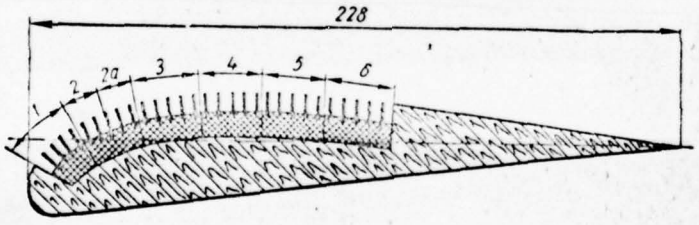

Fig. 2. Flap with plug-ins unit.

Page 257.

If at the flap angle $\delta = 30°$ was obtained the diagram/curve of nonseparated flow, then at $\delta = 35$ and $40°$ is already is distinctly visible the zone of detached flow (according to static pressure

distribution). With $\delta = 45^\circ$ breakaway begins almost from the spout of flap. In thissame mode/conditions were establish/installed two sections of vortex formers (second group of vortex formers), which will lead to the complete liquidation of breakaway. Let us note that the nonseparable character of flow was recorded both behavior of the stuck on the surface of flap silk threads and by the distribution of pressures according to the surface of flap. Both methods give the coinciding results.

As a rule, the unit of sections of vortex formers it leads to the liquidation of breakaway on flap and respectively to an increase in the evacuation/rarefaction above the wing.

From the analysis of summary charts (Fig. 3), where are represented the curves of dependences $\Delta C_y = f(\delta)$ for different types of vortex formers it follows that their effectiveness in many respects depends on the coordinate of the beginning of the region of ribbing. Consequently in order to attain the maximum benefit from the setting up of system of vortex formers, necessary its coordinate it will begin to arrange/locate somewhat higher than the zone of probable flow breakaway. Until now, the coordinate is determined by empiricism (selection). It is clear that if it is located too highly, i.e., in convergent part, this will lead to braking flow, that sharply it will lower effectiveness, but if in the zone of knowingly

detached flow, then vortex system to conceive itself it will not be able, since about vortex former flow irregular slack flow with random return currents.

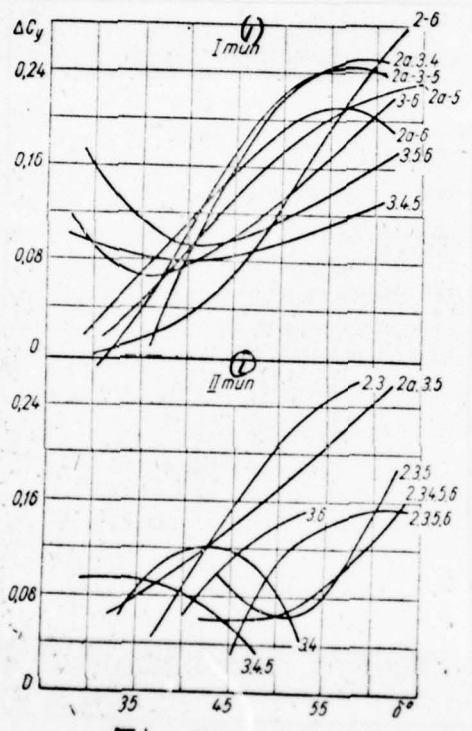

Fig 3

Fig. 3. Summary charts of dependences.

Key: (1). type.

Page 258.

The early beginning of ribbing (from the second section) gives the greatest effect at angles of deflection δ = 50-60°, more rear arrangement of the first finned section (for example, 3-1) it makes it possible to obtain effect at δ = 30-45°. Besides this, it is possible to select the arrangement of the ribbing, which will be "all-system", i.e., gives lift increment with the simultaneous liquidation of separation mode/conditions at all flap angles, exceeding 30°. For the smaller angles of measurement they are not made, since such mode/conditions are usually nonseparable, especially for a slotted flap.

In this case, apparently, will justify itself the application/use of two series of vortex formers, when the second series is arrange/located in the zone of probable breakaway after the first series, i.e., when between both series there is the section of smooth surface.

Being based on the results of the experiments, made earlier, to

that which was given above it is possible to add that the transverse size/dimensions of vortex formers substantially do not change during a change in the geometric scale of model. Size/dimensions of vortex formers depend mainly on the speed of the flow, which flows around vortex formers. One should expect that for rates 40-60 m/s the optimum size/dimensions will turn out to be one order those which were accepted in experiment. The results of experiment one should consider faster as qualitative, than quantitative since it it was not model. This is explained themes that the size/dimensions of model for a working section were overstated as a result of the need for obtaining the sufficiently large flap, on which it would be possible to place vortex formers of the necessary size/dimensions and possibly more drain holes. Under these conditions entire/all air jet, which escape/ensues from nozzle, is deflect/diverted by model.

One should expect that with the observance of the model nature of evacuation/rarefaction on the suction side of wing and flap they will be much greater than this obtained in experiment; however, breakaway, possibly, it will begin somewhat earlier. As a whole it is possible to assume a noticeable increase in the effectiveness of vortex formers.

Theoretical and experimental data confirm that during the nonseparable and even flow of bodies of airflow the frictional

resistance will be less, if boundary-layer flow laminar, and vice versa, if with the same Reynolds numbers is establish/installed turbulent flow, then frictional resistance it increases with an increase in the turbulence level.

By our experiments it is shown, that it is possible to attain a reduction/descent in the frictional resistance during turbulent boundary-layer flow. A reduction/descent in the resistance is achieved by the creation of the local separation zones, in which the averaged rate is substantially lower than the rate in external flow.

Page 259.

Local separation is created as a result of the flows of vortex formers, which are oriented perpendicular to external flow.

After vortex former is formed the vortex sheet, and therefore velocity diagram of surface of the streamlined body (h = 15 mm, b = 10 mm, distance 80 mm) it is transformed in such a way that on very body surface has characteristic for the so-called stagnation zone the section of low speeds with the small gradients of rate (Fig. 4).

For testing the position mentioned above was carried out weight

experiment in wind tunnel for the purpose of research on effect of vortex formers on the drag data of bodies, which were being located in airflow.

By the subject of investigation selected body of revolution 80 mm in diameter (Fig. 5), which will ensure the exception/elimination of end effects. The model of body of revolution consists of forepart/nose, cylindrical and end parts. Nose has spherical form. The length and the conicity of the tail piece of the body of revolution is selected in such a way that it was possible to avoid the separation phenomena, especially with small Reynolds numbers.

In the cylindrical part of the body of revclution was arranged vortex former, which it is located from the beginning of model at a distance 80 mm. The speed of flow in wind tunnel varies within the limits 0-35 m/s.

The drag of body of revolution is measured with the aid of aerodynamic balances. The suspension of the model of body of revolution to to aerodynamic balances is realize/accomplished with the aid of string d = 0.2 mm, that eliminated the effect of suspensions on the drag of body of revolution.

The agreement of the longitudinal axis of the body of revolution

and direction of the speed of flow is checked by the measurement of lift with the aid of aerodynamic balances. In this case the lift was equal to zero.

According to the results of experiment were constructed the graph/diagrams of the dependence of the drag coefficient of body of revolution on Reynolds number for the varied conditions of flow (Fig. 6).

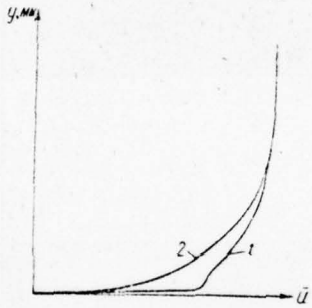

Fig. 4. Diagram/curve of speed $y = f(\bar{u})$ for smooth surface (1). after vortex former (2).

The drag is determined for the model of body of revolution with smooth surface, separately with horse collar d = 0.4 mm and separately with vortex former with ratio h/b = 1.5, where h are a depth and b is width of vortex former. Were carried out also experiments regarding drag during the joint installation of horse collar and vortex former.

The comparison of the drag coefficient of body of revolution with the smooth surface and of drag coefficients with vortex former and by vortex generator indicates a noticeable reduction/descent or an increase in the drag coefficient in the latter case. Figure 6 shows, that during the installation of horse collar at a distance 40 mm from the beginning of the cylindrical part of the body of revolution the drag will be more than resistance for a smooth surface with Reynolds numbers $7 \cdot 10^5 - 1.3 \cdot 10^6$.

During the simultaneous installation of horse collar and vortex former with Reynolds numbers $4 \cdot 10^5 - 10^6$ the resistance sharply decreases in comparison with resistance for a smooth surface and only with Reynolds numbers from 10^6 to $1.3 \cdot 10^6$ the resistance of body of revolution becomes temporarily more than for a smooth surface.

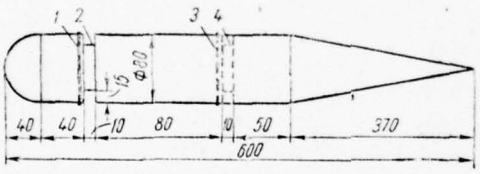

Fig. 5. Model of the body of revolution with the cylindrical form of the nose: 1 - vortex generator No 1; 2 - vortex former No 1; 3 - vortex generator No 2; 4 - vortex former No 2.

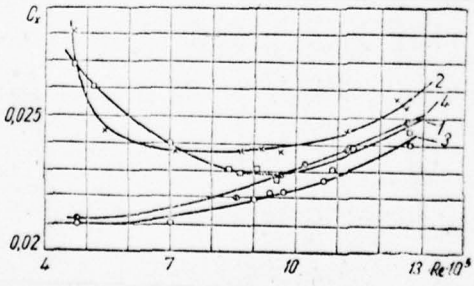

Fig. 6. Graph/diagram of dependence C_x = f (Re): 1 - smooth surface; 2 - vortex generator No 1; 3 - vortex former No 1; 4 - vortex generator No 1 and vortex former No 1.

Page 261.

The resistance of body of revolution with vortex former in all range of the numbers of Reynoldss (from $4 \cdot 10^5$-$1.3 \cdot 10^6$) remains smaller in comparison with the resistance of body of revolution with smooth surface, and is also less than during joint installation vixreobrazovatel6-vortex generator.

Figure 7 gives the results of the experiments, made for the very adverse conditions, when after the first vortex former at a distance 80 mm was arranged horse collar d = 0.4 mm.

The presence of this vortex generator noticeably increased the resistance of body of revolution (curve 1); however, during discovery/opening of vortex former arrange/located directly behind vortex generator, the drag of body of revolution decreases approximately to the initial.

For the study of the effect of the size/dimensions vortex former on drag was made the model of body of revolution whose length is 710 mm whose diameter is 80 mm with parabolic form of nose. The construction of vortex former will make it possible to change the width of the latter within limits b/h = 5-0.5, where b are width, h is a depth of vortex former (h = const = 5 mm). Vortex former was

establish/installed at a distance 60 mm from the beginning of the cylindrical part of the body of revolution. The experimental proceedure is the same as for the first model.

The results of investigations are given in Fig. 8, where is shown the dependence of drag coefficient on Reynolds number and size/dimensions of vortex former.

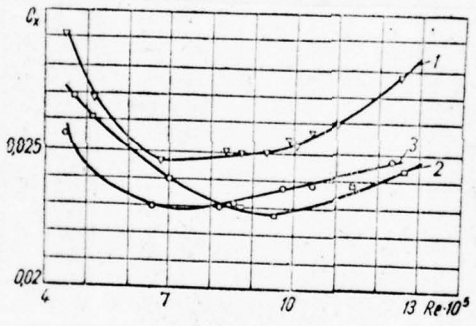

Fig. 7. Graph/diagram of dependence C_x = f (Re): 1 - vortex former No 1 and vortex generator No 2; 2 - smooth surface; 3 - vortex former No 1 and No 2 and vortex generator No 2.

Page 262.

With ratio b/h = 5-3 and Reynolds numbers $4 \cdot 10^5$-$1.2 \cdot 10^6$, the resistance of body of revolution with vortex former is more than for a smooth surface. With ratio b/h = 2.5-2 and Reynolds' numbers $4 \cdot 10^5$-$8 \cdot 10^5$, the resistance of body of revolution with vortex former sharply decreases and becomes less than for a smooth surface, and only with large Reynolds numbers resistance becomes greater than for a smooth surface.

The resistance of body of revolution with vortex formers, relative size/dimensions of which b/h = 1.5-0.5, will render/show smaller than for a smooth surface with all range of Reynolds numbers.

The smallest resistance of body of revolution will render/show with the relative size/dimension of vortex former b/h = 0.8. With the further decrease b/h the resistance of body of revolution with vortex former will increase. Figure 9 gives the dependence of the increase of drag coefficient from the relative size/dimension b/h for different Reynolds numbers.

By analyzing the obtained dependences, it is possible to show that with an increase in the relative size/dimension b/h the increase of drag coefficient decreases.

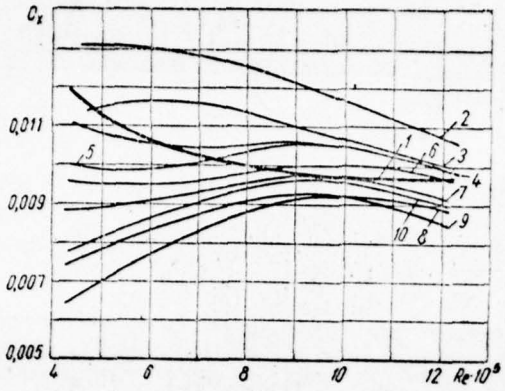

Fig. 8. Graph/diagram of dependence C_x = f (Re, b/h): 1 - the smooth body surface of rotation; 2 - vortex former b/h = 5 (h = 5 mm); 3 - b/h = 4; 4 - b/h = 3; 5 - b/h = 2.5; 6 - b/h = 2; 7 - b/h = 1.5; 8 - b/h = 1.0; 9 - b/h = 0.8: 10 - b/h = 0.5.

Page 263.

The maximum gain of drag coefficient is achieved at b/h = 0.8 in the range of Reynolds numbers $4 \cdot 10^5$-$1.2 \cdot 10^6$. With small Reynolds numbers ($4 \cdot 10^5$-$8 \cdot 10^5$) the increase of the drag coefficient is more intense than for Reynolds numbers from $8 \cdot 10^5$ to $1.2 \cdot 10^6$.

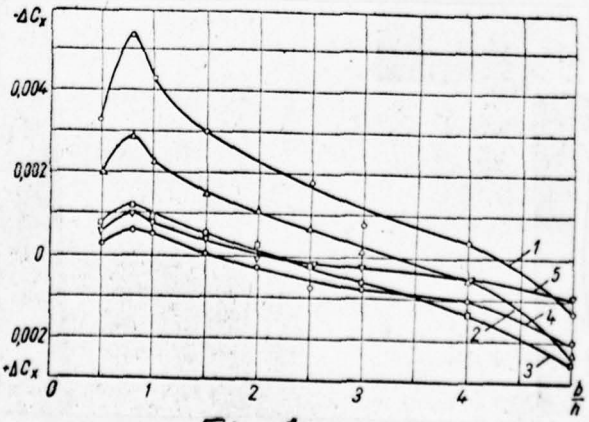

Fig. 9.

Fig. 9. Graph/diagram of dependence $\Delta C_x = f(\mathrm{Re}, \frac{b}{h})$: 1 - Re = $4.4 \cdot 10^5$; 2 - $6 \cdot 10^5$; 3 - $8 \cdot 10^5$; 4 - 10^6; 5 - $1.2 \cdot 10^6$.

BIBLIOGRAPHY

1. Блохинцев Д. И.— Возбуждение резонаторов потоком воздуха, ЖТФ, 1945, 15, 1-2.
2. Кубанский П. Н.— ЖТФ, 1957, 27, 180.
3. Кубанский П. Н.— ЖТФ, 1952, 22, 9.
4. Мигай В. К.— Изв. АН СССР. ОТН. Механика и машиностроение, 1960, 4.
5. Мигай В. К.— В кн.: XIV научно-техническая сессия по проблемам газовых турбин. М., 1961.

ELECTRICAL SIMULATION OF THE FLOW AROUND OF THE WINGS OF INFINITE SPAN AND MAGNETIC SIMULATION OF FINITE-SPAN WINGS.

G. A. Ryazanov.

(Leningrad).

Page 264.

The electrical simulation of flat/plane circulatory flows can be based on straight line and indirect electrohydrodynamic analogies. In the first case of speed corresponds the strength of stationary electric field in conducting medium

$$v_x \to E_x; \quad v_y \to E_y, \tag{1}$$

in the second - the vector, to equal vector E in value, but component with it angle 90°:

$$v_x \to E_y; \quad v_y \to -E_x. \tag{2}$$

Respectively the airfoil/profile of body they simulate by dielectric or supplementary electrode [9]. The direct/straight analogy makes it

possible more accurately to determine speeds on the airfoil/profile of body and is preferable.

Since the circulation flow of liquid does not have direct/straight analog in the electric field, created by electrodes, usually it they reproduce artificially with the aid of supplementary busbar/tires, which seriously complicates experiment [9, 11, 12]. This it is possible to avoid, if we use the vortex/eddy electric field, which surrounds the toroidal electromagnet whose winding is included in alternating current circuit [3, 4]. When using the conducting plates electromagnet they insert in the hole, which imitates airfoil/profile, and excited by it in conducting medium induction electric field it serves as the natural analog of circulatory flow. Model turned out to be that which was coupled with alternating/variable magnetic flux and forms seemingly secondary winding of step-down transformer.

Page 265.

In this case the effective value of circulation integral of the vector E on any duct, which covers airfoil/profile, has constant value. By regulating current strength in the magnetizing magnet winding, it is possible to satisfy the condition of zhukovskiy - Chaplygin, as criterion of whom serves the bias of the second

critical point to trailing edge or the equality of the speeds on the upper and lower sides of wing in infinitely close to it points.

Electrohydrodynamic analogy is spread only to the region, occupied with conducting medium, and therefore the eddy/vortex of electric field, localized in magnet core, it is not the analog of the connected vortex flow of liquid. The question is only compiling circulation integral of the vector E around airfoil/profile, the position of electromagnet not having a value. Its displacement/movement within airfoil/profile does not change the coupled with model magnetic flux and, consequently, also the structure of electric field. Boundary conditions on airfoil/profile, circulation integral of the vector E and the strength of undisturbed field in this case do not change.

The realization of zhukovskiy - Chaplygin's condition without supplementary electrodes makes it possible to apply as conducting medium the plates of aluminum foil [1] considerably more uniform, than electro-conductive paper, and substantial to raise the accuracy of the measurements of field.

FOOTNOTE [1]/. is utilized the released by industry foil, glued to paper (" masked" on paper). ENDFOOTNOTE.

In the department of physics of the LIVTa developed device (electro-integrator of rotational field), which makes it possible to investigate on one plate of foil 200 x 50 cm in size/dimension the circulation flow about the winged airfcil/profile in unrestricted flow at angles of attack 0 and 90°. This is achieved by a change in the direction of the external field, which imitates the incident flow, whereupon the effect of the boundary/interfaces of plate with airfoil chord into 40-50 cm virtually is eliminated.

Combining data of these two experiments, it is possible to obtain the distribution of relative speed for any assigned angle of attack

$$v^0 = \frac{E_\parallel}{E_{0\parallel}} \cos\alpha + \frac{E_\perp}{E_{0\perp}} \sin\alpha, \qquad (3)$$

where $E_\parallel$ and $E_\perp$ are electric intensities on airfoil/profile during the longitudinal and transverse feed modes of model, a $E_{0\parallel}$ and $E_{0\perp}$ are the corresponding to them strength of the undisturbed field,

measured before the formation of hole. Analogous with this the dimensionless circulation is determined by the relationship/ratio

$$\Gamma^0 = \frac{\mathcal{E}_{\parallel}}{lE_{0\parallel}} \cos\alpha + \frac{\mathcal{E}_{\perp}}{lE_{0\perp}} \sin\alpha, \qquad (4)$$

where $\mathcal{E}_{\parallel}$ and $\mathcal{E}_{\perp}$ - the corresponding electromotive forces, which appear in the duct, coupled with magnet core, but l is a chord of the hole, which imitates airfoil/profile.

Page 266.

Schematic diagram is shown in Fig. 1, where B - are switches, P - joints, Л1 - the plate of foil, Э - electromagnet, e - electrodes, R - the resistance of channels, and ДЗ is a double probe for the measurement of the strength of field. With the aid of the pressing steel frame, on which are fastened the isolated/insulated from it evenly distributed brass electrodes e, against the plate of aluminum foil Л1 is pressed framework abcd from the copper wire whose diameter is selected depending on the thickness of foil, whereupon consecutively with electrodes e is included resistance R, by two or three of order exceeding the specific skin drag of foil. In the

middle of the conducting plate is cut out the hole, which imitates airfoil/profile so that its chord would be parallel to edges bc and ad. After include/connecting model in circuit with the aid of the electrodes, arrange/located along sections ab and ~~CD,~~ cd, they reproduce the flow about the airfoil/profile at angle of attack 0°. In this case the electrodes, established/installed along sides bc and ad, disconnect from external circuit, and are utilized these sections of the framework only for the elimination of the effect of the boundary/interfaces of the conducting plate.

Since the resistance of copper wires has the same order, as the resistance of the plate of foil, and they consume considerable current, them they connect to the terminals of external circuit with the aid of the wires of the same cross section whose length is regulated so that the contact of the wire framework with the conducting plate before the formation of hole would not disturb the uniformity of electric field.

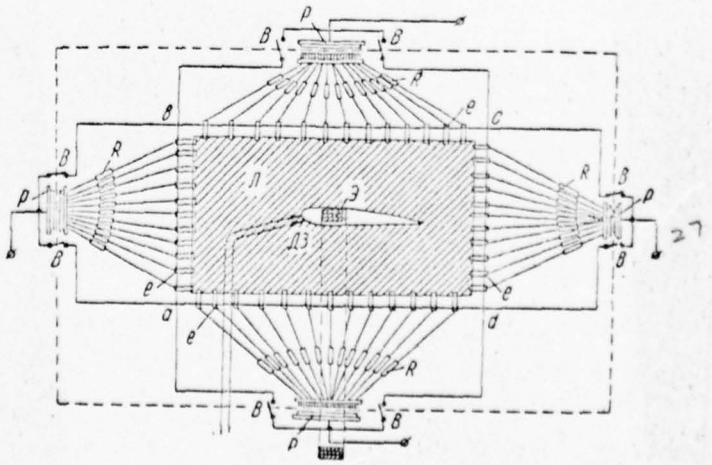

Fig. 1.

Page 267.

For this the ratio of the length of lead wires to the length of sides bc and ad must be equal to the ratio of the total resistance of the feeding channels R to the resistance of the conducting plate.

Then the electrodes, arrange/located along sections ab and ~~CD~~ cd, disconnect from the terminals of external circuit, and instead of them they connect the electrodes, arrange/located along the longitudinal sides bc and ad. Since they are included consecutively with equal resistance and currents in their channels are equal, in the rectangular conducting plate appears the uniform the electric field, which corresponds to the incident flow at the angle of attack of airfoil/profile 90°. Wires bc and ad smooth the discrete character of feed/supply. And in this case the wire framework abcd compensates for the effect of the boundary/interfaces of the foil: its transverse sides are included in circuit with the aid of the wires of the same cross section, whereupon the ratio of their length to the length of sides ab and ~~CD~~ cd must be equal to the ratio of the total resistance of channels R to the resistance of model in this feed mode.

Figure 2 gives the chord diagrams of relative speed for airfoil/profile NACA 4412, obtained in one of the control experiments.

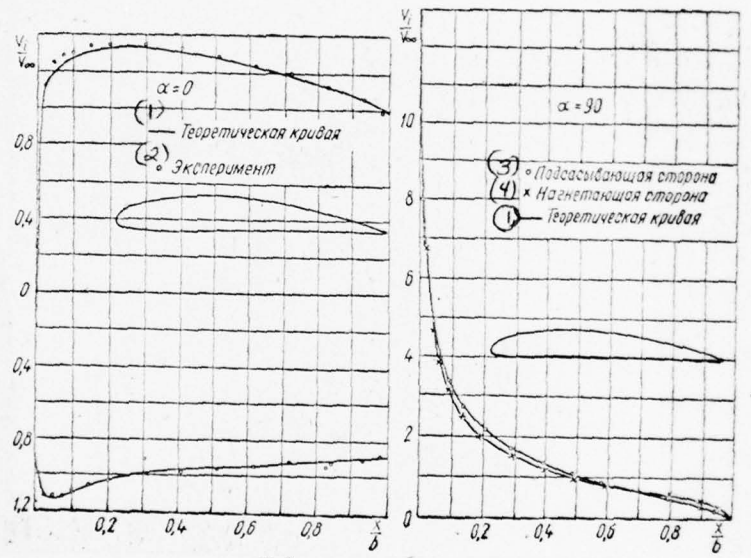

Fig. 2.

Key: (1). Theoretical curve. (2). Experiment. (3). Sucking side. (4). Forcing side.

Page 268.

Figure 3 shows the grid of field at angle of attack 90°.

The described device makes it possible to simulate the flow about the airfoil/profile near solid wall and free surface of liquid. The procedure, based on the application/use of a vortex/eddy electric field, makes it possible also to consider boundary layer effect, to simulate the flow about the annular wing (guide of nozzle) and the flow about the airfoil cascade [1].

It is known that if we in the region, occupied with alternating/variable magnetic flux, arrange the conducting plate, then in it will arise eddy currents. Them causes vortex/eddy electric field. In the circular and uniform plates, placed in uniform magnetic field it is normal to its lines of force, the strength of induction quasi-stationary electric field will satisfy linear law, and this field can imitate the incident flow during the rotation of

airfoil/profile in ideal fluid. Cutting out in this plate the hole, similar to airfoil/profile, so as to the center of plate would coincide with center of rotation, we will obtain the model of the turned flow. There is a possibility to separate its potential component, created by the induced quasi-stationary charges, and, after measuring the caused potentials, to find the connected moment of the inertia of body [2, 5]. During the study of the flow about the winged airfoil/profile into hole is inserted the toroidal electromagnet (3), which has two windings (magnetizing and compensating for external magnetic field), and with the aid of its rotational field is satisfied zhukovskiy - Chaplygin's condition (Fig. 4). For the elimination of the effect of the external edges of model is applied two circular plates, isolate/insulated from each other by an entire area, but connected by their edges. The potential component of electric field in lower plate will serve as the conformal mapping of the exterior of indused field.

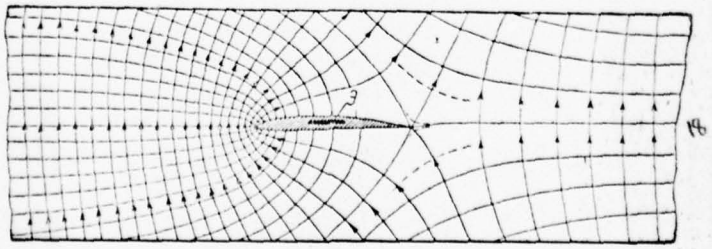

Fig. 3.

The described method makes it possible to reproduce the turned flow during the translational-rotational motion of airfoil/profile (flow about the airfoil/profile of cycloidal propeller). It suffices to misalign the center of rotation of airfoil/profile relative to the center of plate to the distance, which corresponds to the relative angular velocity, equal to the ratio of airfoil chord to radius of a circle, described by center of rotation.

However, at the low relative speed of airfoil/profile is required a decrease in the chord of hole, and then procedure changes. The center of gravity of airfoil/profile is combined with the center of plate, and on the vortex/eddy electric field, created by external magnetic field, is placed the cophasal with it uniform potential field, which corresponds to the incident flow during the forward motion of body. This is reached with the aid of the point electrodes, placed on the edges of plate and connected through equal resistance, by 2-3 orders exceeding the specific skin drag of plate. The equality of the currents, entering the model, makes it possible to carry out on its duct the distribution of the function of flow, which corresponds to uniform field. For this the circumference of plate they divide/mark off into even number of sections with the aid of the equidistant straight lines, the parallel to the assigned direction of field, and at the points of its intersection with odd straight lines are establish/installed electrodes (Fig. 5). After determining the

speed of the turned flow, it is possible to find corresponding to them pressure distribution.

In the physical laboratory of LIVTa is installation, in which the vortex/eddy zone of induction electric field create Helmholtz' rings 1.5 m in diameter and are applied the plates of foil 1 m in diameter. By utilizing a vortex/eddy zone of induction electric field, the external vortex/eddy electric field of toroidal electromagnets and the potential electric field, created by electrodes, it is possible to construct the model of radial grid/cascade.

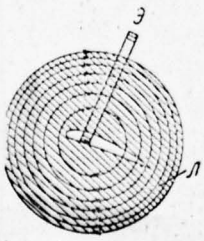

Fig. 4.

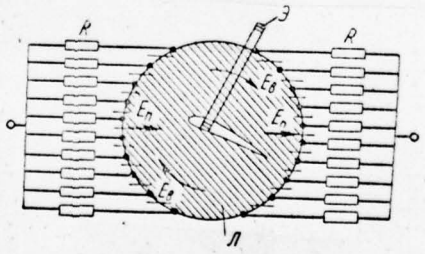

Fig. 5.

Page 270.

Outside the region, streamlined with current, magnetic field has the single-valued potential ξ, which satisfies the equation of Laplace, and it can serve as the mathematical model of the flow of ideal fluid. By the analog of speed is the magnetic induction (vector B) or magnetic field strength (vector H), the analog of velocity potential, i.e., the corresponding to them magnetic potentials. During the study of the field of vortex/eddy system this analogy makes it possible to replace cumbersome calculations according to the law of bio - savart with simple experiment by the model, which is the geometrically similar system of currents [8], the magnetic field can be constant or variable.

Magnetostatic field (or the alternating magnetic field of commercial frequency) can be used also for the simulation of the streamlined bodies. In this case as the analog of the velocity field serves the field of vector H in the ferromagnetic plate, which has large relative magnetic permeability, with the hole, geometrically similar to the airfoil/profile of body [9]. This model makes it possible to reproduce the circulation flow about the airfoil/profile; however, this experiment is very complex and during the study of incompressible flows cannot compete with electrical simulation, based on the application/use of a vortex/eddy electric field. The

application/use of a ferromagnetic medium for the solution of three-dimensional problems encounters even larger difficulties. At the same time the condition of nonpassage logically is realized in three-dimensional magnetic field, if we the model of body fulfill from the well conducting material (copper, aluminum), and field frequency to raise to dozens kilohertz [7, 10]. As a result of surface effect (skin effect) the alternating magnetic field of supersonic frequency virtually does not penetrate the metal with high conductivity and on the surface of model is made the boundary condition

$$B_n = 0, \quad (5)$$

similar to the condition of nonpassage on solid wall. A good conductor almost so we nonpenetrate for a high-frequency magnetic field as solid body for a fluid flow.

The models of the streamlined bodies can be hollow; sufficiently in order that wall thickness would reach 1 mm. Them it is possible to prepare by the method of electrolytic plating, with the aid of casting or from copper sheet. During the manufacture of the duplicated/backed up/reinforced model of vessel it is possible to combine casting from aluminum and the application/use of the latten: cylindrical insert is made from copper sheet (ccpper it is bended out on the wooden template/pattern, which for a strength remains within

model)., and nose and forages - by casting. Aluminum parts are copperplated in plating bath and are fixed on to copper. The models of finite-span wings are made analogously.

The magnetic simulation of three-dimensional flows has a series of essential advantages in comparison with experiment in electrolyyic bath.

Page 271.

The point induction sensor of magnetic field with three coils allows all three velocity component, and linear (Rogowski loop) is its potentials. On the surface of the model of body it is possible to construct the lines, similar to flow lines and to the lines of equal velocity potential; it is possible to determine fluid flow rate through the surface, limited by the assigned duct; derivative of speed in the direction; the caused potentials, etc.

Measurements conduct in air, and their accuracy/precision can be high.

If the conducting model of finite-span wing is placed in the external uniform magnetic field of supersonic frequency at the assigned angle of attack, then the eddy currents, induced in its

surface layer, will be the analog of the bound vortexes, which replace by themselves wing in fluid flow during its noncirculating flow. Their surface density i_1, equal with an accuracy to constant factor the surface rotor of magnetic field and connected with magnetic induction on the surface of model B_1 by the relationship/ratio

$$\vec{i}_1 = \frac{1}{\mu} \vec{\mathrm{Rot}} B_1 = \frac{1}{\mu} [\vec{n} \vec{B}_1], \qquad (6)$$

where μ - magnetic permeability of medium, n - external standard, will serve as the analog of the intensity of the bound vortexes

$$\vec{\gamma}_1 = \vec{\mathrm{Rot}} v_1 = [\vec{n} \vec{v}_1], \qquad (7)$$

where v_1 - speed on wing surface during its noncirculating flow.

Subsequently with the explanation of the proposed procedure of simulation let us call these surface eddy/vortices - first-order

bound vortexes.

From (7) it follows that if we on wing surface conduct arbitrary curve, then at any point of it the projection of vector on the direction of standard to this curve (N), that lies at the plane of tangent to wing surface, is equal to the projection of speed on the direction of curve (L):

$$\gamma_{LN} = v_{LT}. \quad (8)$$

whereupon unit vectors $\vec{L}$ and $\vec{N}$ form with vector $\vec{n}$ right-handed system. Similar relationship/ratio is fulfilled with the magnetic model of the wing:

$$i_{LN} = \frac{1}{\mu} B_{LT}. \quad (9)$$

This means that, after constructing into the surfaces of the model of the wing of the line of equal magnetic potential, which differ by

constant interval $\Delta\xi$, we will break it into the strips, which correspond to equal to the circulation $\Delta\Gamma$, each of which can be identified with the concentrated vortex line of constant intensity.

Page 272.

The speed on wing surface and the magnetic induction on the surface of its magnetic model are determined by the relationship/ratios

$$\vec{v}_1 = [\vec{\gamma}_1 \vec{n}]; \quad \vec{B}_1 = \mu [\vec{i}_1 \vec{n}]. \qquad (10)$$

The eddy currents, which appear in the surface layer of model, are distributed so that their field compensates for external uniform field in the region, occupied by the model, in the same way as the field first-order of bound vortexes compensates for the incident flow within body. Just as first-order bound vortexes, these currents are closed on the surface of the model of wing, and in magnetic field there is not no one duct, for which the circulation integral of the vector B would be different from zero. In the space, which surrounds model, the field of these currents it has single-valued potential and

serves as the analog of the caused flow.

If the magnetic model of the noncirculatory flow about a wing of the final spread/scope directly reflects the main features of nature, then during the simulation of three-dimensional circulatory flow the situation is otherwise. In magnetic field there are no factors, which lead to satisfaction of the condition Jcukowski-of Chaplygin and emergence of the film of free vortices. In order to achieve here the mathematical analogy of the phenomena, it is necessary artificially to create the vortex/eddy system of magnetic field, similar to vortex sheet and its closing bound vortexes (let us call them second-order bound vortexes), having forcedly subordinated to its laws, which logically appear in fluid flow. In this case the film of free vortices mentally replaced by discrete vortex lines.

Since by the magnetic analog of free vortex flow of liquid conducts with current, to the coming out edge of the model of wing they connect wiring system, having in pairs connected them to the external (independent variable) voltage sources. The resistance of the model of wing vanishingly little in comparison with the resistance of any pair of these wire/conductors and, by regulating external voltages (on value and phase), it is possible to reproduce in space any distribution of free vortices $\vec{\gamma}_{св}$. In this case the external current, which flows in the model of wing (in its thin

surface layer), will serve as the analog of bound vortexes.

Let us assume which is required to reproduce flow around of the wing with the rounded end/faces (Fig. 6) on the assumption that free vortices converge only from its trailing edge and are directed along the incident flow.

Page 273.

In this case the wire/conductors, which imitate vortex sheet, line along the lines of force of external uniform magnetic field, and as the criterion of the realization of zhukovskiy - Chaplygin's condition serves the equality of the normal (to trailing edge) components of vector B at two infinitely close points on the upper and lower sides of the model of wing. In order to fulfill this requirement, on the upper and lower sides of the model of wing in immediate proximity of its trailing edge and of each other establish/install two identical induction sensors, the planes of coils of which are parallel to trailing edge. During their connection consecutively so that appearing in them emf would be directed oppositely, they form the differential transmitter whose readings on symmetrical model at zero angle of attack must be equal to zero. With an increase in the angle of attack the output potential of this sensor will grow/rise, having the greatest value in maximum cross

section of model. Sensor is establish/installed against the points, which lie accurately in the middle between wire/conductors and by successive approximation are selected in them such currents, by which its readings are everywhere equal to zero. The values of these currents make it possible to judge the distribution of dimensionless circulation according to spread/scope. Figure 7 gives the results, obtained for the wing, shown in Fig. 6.

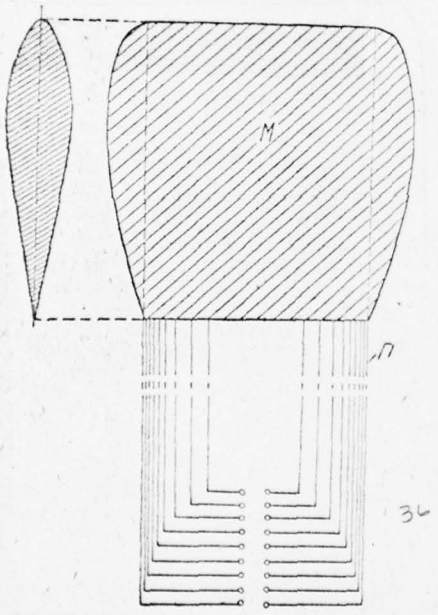

Fig. 6.

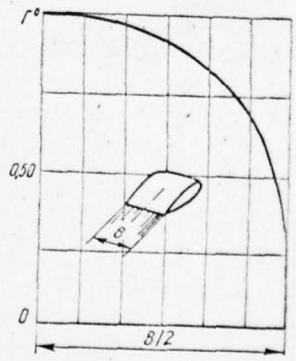

Fig. 7.

Page 274.

Vector B on the surface of model measure with the aid of the induction sensor, which contains two mutually perpendicular coils and relate its values to the induction of the undisturbed uniform magnetic field. The obtained on them pressures are close to the results of blasting in wind tunnel. Agreement becomes even more complete, if we imitate free vortices, which descend from the end/faces of wing, after selecting the appropriate currents from the condition of the equality of zero compcnent of vector B, normal to the line of the descent of these eddy/vortices. During the simulation of flat-topped wing their effect becomes essential.

For transfer to the nonlinear formulation of the problem, it is necessary to change the form of wire/conductors in order that at the indicated above points, besides the equality of zero components of vector B, normal to trailing edge, and the corresponding condition on end/faces, would occur the equality of vectcrs B on module/modulus. Furthermore, it is necessary to carry out equality zero of normal

component of vector B on an entire surface, which imitates vortex sheet.

By utilizing flat/plane latten, it is possible to simulate flow around of the wing near screen.

By the department of physics of LIVT is developed the device, in which the range of uniform of magnetic field has a volume of approximately 5 m³, and vortex sheet they imitate 20 wire/conductors (their number can be increased).

Bibliography

1. Рязанов Г. А.— В кн.: Экспериментальная гидромеханика судна, 56. Изд. НТО СП, Л., 1964.
2. Рязанов Г. А.— В кн.: Труды межвузовской конференции по применению физического и математического моделирования в различных отраслях техники. Изд. МЭИ, М., 1962.
3. Рязанов Г. А.— Изв. АН СССР. ОТН. Механика и машиностроение, 1961, 3.
4. Рязанов Г. А. Авт. св. № 148279, 1962 г.
5. Рязанов Г. А. Авт. св. № 148280, 1962 г.
6. Рязанов Г. А. Авт. св. № 164441, 1964 г.
7. Рязанов Г. А. Авт. св. № 165556, 1964 г.
8. Рязанов Г. А., Копеецкий В. В. Авт. св. № 168459, 1965 г.
9. Сунцов Н. Н. Методы аналогий в аэрогидродинамике. Физматгиз, М., 1958.
10. Тетельбаум И. М., Баяковский Ю. М., Авт. св. № 137277, 1961 г.
11. Фильчаков Н. И., Панчишин В. И. Интеграторы ЭГДА 6/51 и ЭГДА 6/53. Изд-во АН УССР, К., 1961.
12. Malavard L., Hacques G.— В кн.: Adv. in Aeronaut. Sci., 2. Pergamon Press, 1959, pp. 771—796.

UNCLASSIFIED

SECURITY CLASSIFICATION OF THIS PAGE *(When Data Entered)*

REPORT DOCUMENTATION PAGE		READ INSTRUCTIONS BEFORE COMPLETING FORM
1. REPORT NUMBER FTD-ID(RS)T-0784-77	2. GOVT ACCESSION NO.	3. RECIPIENT'S CATALOG NUMBER
4. TITLE *(and Subtitle)* HYDRODYNAMICS OF LIFTING SURFACES (SELECTED ARTICLES)		5. TYPE OF REPORT & PERIOD COVERED Translation 6. PERFORMING ORG. REPORT NUMBER
7. AUTHOR*(s)*		8. CONTRACT OR GRANT NUMBER*(s)*
9. PERFORMING ORGANIZATION NAME AND ADDRESS Foreign Technology Division Air Force Systems Command U.S. Air Force		10. PROGRAM ELEMENT, PROJECT, TASK AREA & WORK UNIT NUMBERS
11. CONTROLLING OFFICE NAME AND ADDRESS		12. REPORT DATE 1966 13. NUMBER OF PAGES 161
14. MONITORING AGENCY NAME & ADDRESS*(if different from Controlling Office)*		15. SECURITY CLASS. *(of this report)* UNCLASSIFIED 15a. DECLASSIFICATION/DOWNGRADING SCHEDULE
16. DISTRIBUTION STATEMENT *(of this Report)* Approved for public release; distribution unlimited		
17. DISTRIBUTION STATEMENT *(of the abstract entered in Block 20, if different from Report)*		
18. SUPPLEMENTARY NOTES		
19. KEY WORDS *(Continue on reverse side if necessary and identify by block number)*		
20. ABSTRACT *(Continue on reverse side if necessary and identify by block number)* 20		

DD FORM 1 JAN 73 1473 EDITION OF 1 NOV 65 IS OBSOLETE

UNCLASSIFIED

SECURITY CLASSIFICATION OF THIS PAGE *(When Data Entered)*

DISTRIBUTION LIST

DISTRIBUTION DIRECT TO RECIPIENT

ORGANIZATION		MICROFICHE
A205	DMATC	1
A210	DMAAC	2
B344	DIA/RDS-3C	8
C043	USAMIIA	1
C509	BALLISTIC RES LABS	1
C510	AIR MOBILITY R&D LAB/FIO	1
C513	PICATINNY ARSENAL	1
C535	AVIATION SYS COMD	1
C557	USAIIC	1
C591	FSTC	5
C619	MIA REDSTONE	1
D008	NISC	1
H300	USAICE (USAREUR)	1
P005	ERDA	1
P055	CIA/CRS/ADD/SD	1
NAVORDSTA (50L)		1
NAVWPNSCEN (Code 121)		1
NASA/KSI		1
AFIT/LD		1

ORGANIZATION		MICROFICHE
E053	AF/INAKA	1
E017	AF/ RDXTR-W	1
E404	AEDC	1
E408	AFWL	1
E410	ADTC	1
E413	ESD	2
	FTD	
	CCN	1
	ETID	3
	NIA/PHS	1
	NICD	5